Available online at www.sciencedirect.com
ScienceDirect
Bioorganic & Medicinal Chemistry
Bioorganic & Medicinal Chemistry 15 (2007) 2054–2080

Azetidinones as vasopressin V1a antagonists

Christophe D. Guillon,[a,b,*] Gary A. Koppel,[b] Michael J. Brownstein,[b,†] Michael O. Chaney,[a] Craig F. Ferris,[c] Shi-fang Lu,[b,d] Karine M. Fabio,[a] Marvin J. Miller,[e] Ned D. Heindel,[a] David C. Hunden,[f] Robin D. G. Cooper,[f] Stephen W. Kaldor,[f,‡] Jeffrey J. Skelton,[f,§] Bruce A. Dressman,[f] Michael P. Clay,[f] Mitchell I. Steinberg,[f] Robert F. Bruns[f] and Neal G. Simon[b,d]

[a]*Department of Chemistry, 6 East Packer Avenue, Lehigh University, Bethlehem, PA 18015, USA*
[b]*Azevan Pharmaceuticals, Inc., 115 Research Drive, Bethlehem, PA 18015, USA*
[c]*Department of Psychiatry, University of Massachusetts Medical School, S 7-831, 55 Lake Avenue North, Worcester, MA 01655, USA*
[d]*Department of Biological Sciences, 111 Iacocca Hall, Lehigh University, Bethlehem, PA 18015, USA*
[e]*Department of Chemistry and Biochemistry, University of Notre Dame, Notre Dame, IN 46556, USA*
[f]*Lilly Research Laboratories, Eli Lilly and Company, Lilly Corporate Center, Indianapolis, IN 46285, USA*

Received 2 October 2006; revised 15 December 2006; accepted 21 December 2006
Available online 23 December 2006

Abstract—The azetidinone LY307174 (**1**) was identified as a screening lead for the vasopressin V1a receptor (IC_{50} 45 nM at the human V1a receptor) based on molecular similarity to ketoconazole (**2**), a known antagonist of the luteinizing hormone releasing hormone receptor. Structure–activity relationships for the series were explored to optimize receptor affinity and pharmacokinetic properties, resulting in compounds with K_i values <1 nM and brain levels after oral dosing ∼100-fold higher than receptor affinities.

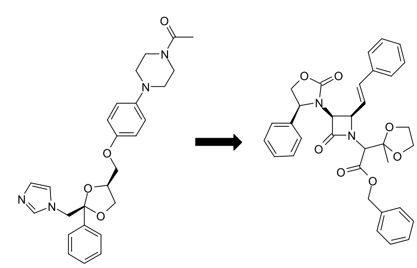

ketoconazole (**2**)
IC_{50} = 2 μM
LHRH receptor

LY307174 (**1**)
IC_{50} = 45 nM
human V1a receptor

1. Introduction

The neurohypophysical hormones vasopressin[1] and oxytocin exert a wide range of physiological effects through binding to specific membrane receptors belonging to the G protein-coupled receptor (GPCR) superfamily. To date, three vasopressin receptor subtypes and one oxytocin receptor have been pharmacologically and functionally described.[1] V1a, V1b, and oxytocin receptors activate phospholipase C, resulting in the production of inositol 1,4,5-trisphosphate and diacylglycerol,

Keywords: Vasopressin; Vasopressin V1a antagonists; Azetidinone; Oral bioavailability; CNS penetration.

* Corresponding author. Tel.: +1 610 758 4706; fax: +1 610 758 6536; e-mail: chg3@lehigh.edu

† Present address: J. Craig Venter Institute, 9704 Medical Center Dr., Rockville, MD 20850, USA.

‡ Present address: Takeda San Diego, Inc., 10410 Science Center Drive, San Diego, CA 92121, USA.

§ Present address: Cargill, Inc., PO Box 5624, Minneapolis, MN 55440, USA.

0968-0896/$ - see front matter
doi:10.1016/j.bmc.2006.12.031

mobilization of intracellular calcium, and activation of protein kinase C. V2 receptors stimulate adenylyl cyclase, resulting in the accumulation of cyclic AMP and activation of protein kinase A. All four receptor subtypes from several mammalian species have been recently cloned,[2–5] as well as closely related receptors from bony fishes and invertebrates.[6,7] Although vasopressin is perhaps best-known for its role in the cardiovascular system, it also has actions in the central nervous system (CNS), and several CNS applications of vasopressin receptor antagonists have been suggested (reviewed in Refs. 8 and 9). A number of research groups have prepared antagonists directed at the vasopressin V1 receptor.[10–15] While V1a antagonists have been made, none of these have been reported to penetrate the CNS efficiently.

2. Results and discussion

Our vasopressin antagonist program was initiated to identify a CNS-active V1a antagonist: one with potent affinity for the human V1a receptor ($IC_{50} < 10$ nM), good oral availability, and ability to penetrate the blood brain barrier—in short, a candidate for human clinical development targeting CNS disorders. The program began at Lilly in 1990 with the selection of a 1500-compound 'Neuropeptide Cassette'—a library intended to identify nonpeptide ligands for neuropeptide receptors. The library applied the concept of receptor crosstalk—previously well documented for the biogenic amine subfamily of GPCRs—to the neuropeptide receptors. The underlying concept is illustrated in Figure 1. Suppose there are two related receptors, A and B. Over the course of evolution, the two receptors have remained identical in part of the binding site (shown as the semicircular portion), while in the rest of the binding site the two receptors have drifted apart due to mutations (shown as the triangular portion in A and the rectangular portion in B). Furthermore, suppose that alpha, a high-affinity ligand for A, is already known, and we wish to find beta, a high-affinity ligand for B. One approach would be to screen all available analogs of alpha in the hope that a mutation in alpha would complement the mutation in A, resulting in a compound with high affinity for B, that is, beta.[16,17]

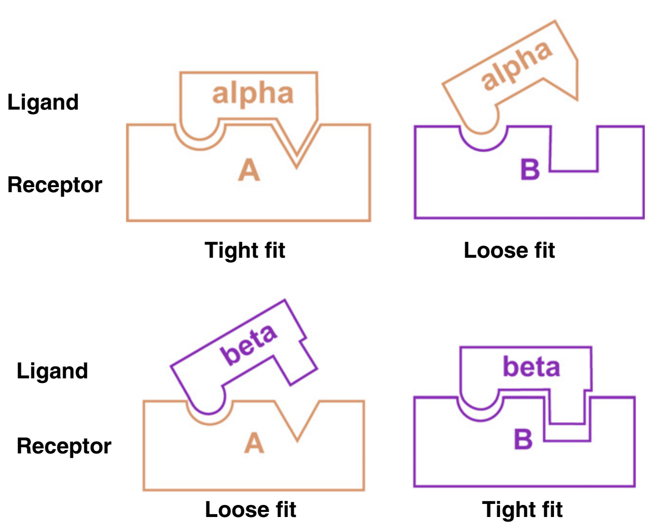

Figure 1. Receptor crosstalk as a screening tool.

In the construction of the Neuropeptide Cassette, 26 known nonpeptide ligands for neuropeptide receptors (cholecystokinin, substance P, angiotensin II, opiate, leuteinizing hormone releasing hormone (LHRH), and motilin receptors) were used in the role of alpha, and molecular similarity searches in MACCS against the 26 alphas were used to identify 'mutated' versions as candidates for beta. Similarity thresholds were adjusted to obtain ~300 matches for each of the 26 query structures, and the ~5000 unique structures selected by this method were reduced to 1500 using the leader clustering method.

Among the 26 query structures was ketoconazole, a marketed antifungal agent known to cause reproductive side-effects due to antagonism of the LHRH receptor.[18] The azetidinone LY307174 (**1**, Fig. 2) was selected for screening based on 59% similarity to ketoconazole (**2**). Compound **1** was found to have an affinity of 45 nM for the cloned human V1a receptor. In agreement with the rationale in Figure 1, some features of **2** such as the dioxolane ring and terminal phenyl are conserved in **1**, while others are totally replaced.

Beyond the simple issue of affinity, **1** was considered an attractive lead for several reasons. LY307174 is a monocyclic beta-lactam (monobactam). Unlike fused-ring beta-lactams such as penicillins and cephalosporins, simple monobactams such as **1** are highly stable to chemical or enzymatic hydrolysis of the four-membered azetidinone ring. The *cis* geometry of the rigid four-membered ring forces the three side-chains together into a fixed geometric configuration, presumably enabling complementarity with sub-pockets of the receptor. Although the molecular weight of **1** is relatively high (568.6), its compactness provided some hope that the series might show significant oral absorption.

After our lead compound was identified, we undertook a structure–activity relationship (SAR) study utilizing the chiral Staudinger 2 + 2 cycloaddition reaction as depicted with a representative example in Scheme 1.

In the sequence in Scheme 1, *trans*-cinnamaldehyde is combined with glycine benzyl ester to form the imine **3**, which is then reacted with the chiral auxiliary acid chloride **4**, to form the four-membered ring **5**. In the example given in Scheme 1, the *S*-chiral auxiliary induces formation of the *R*-*cis* configuration in the azetidinone product. The methylene group of the glycine constituent could be acylated, producing **6**, which displayed potent activity (V1a $IC_{50} = 6.5$ nM). The absolute stereochemistry of the chiral methine carbons of the azetidinone ring of **6**, depicted in Scheme 1, was assigned based on earlier reports on the absolute configuration of these azetidinone carbons produced through the Staudinger 2 + 2 reaction with the Evans' chiral auxiliary.[19,20,25] Confirming this assignment, the analog **7** was crystallized and the absolute configuration determined by X-ray analysis[21] as shown in Figure 3.

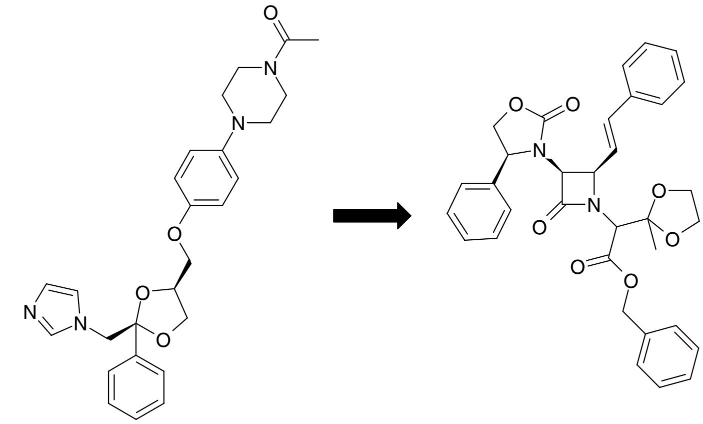

ketoconazole (**2**)
IC_{50} = 2 μM
LHRH receptor

LY307174 (**1**)
IC_{50} = 45 nM
human V1a receptor

Figure 2.

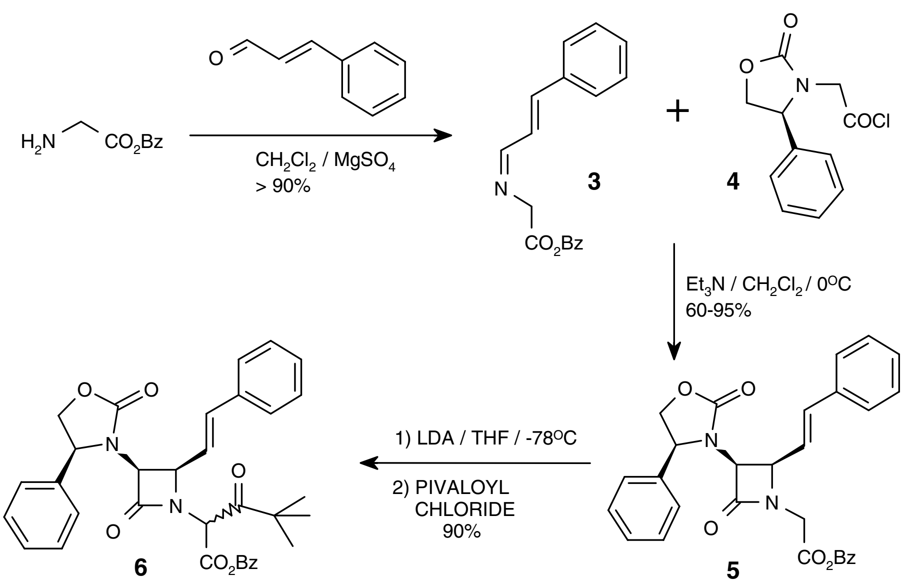

Scheme 1.

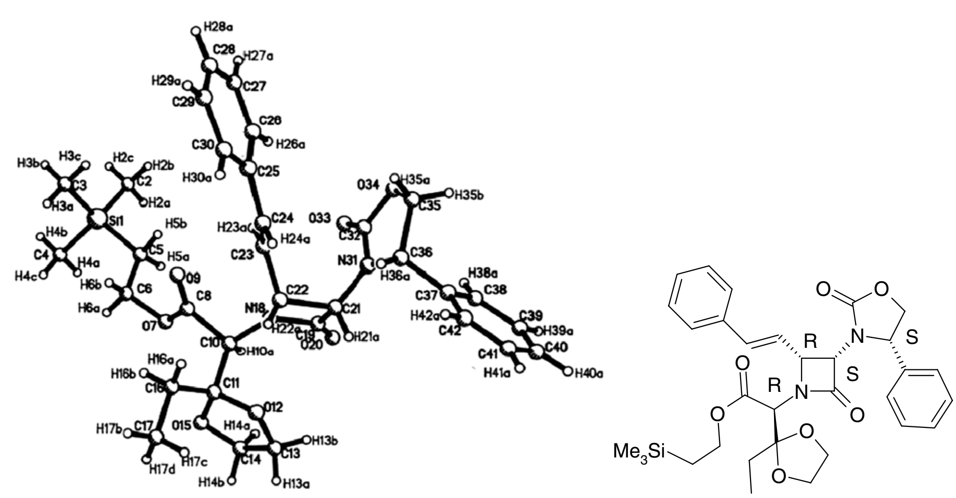

Figure 3. X-ray structure/absolute configuration of **7**.

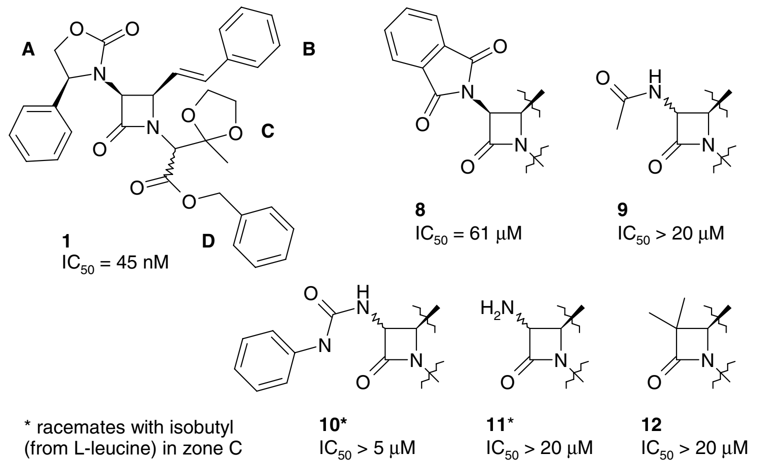

Figure 4. SAR overview of Zone A, 20 compounds prepared.

The SAR strategy was based on the modification of four zones, A–D, of the azetidinone molecule as depicted in Figure 4. A limited SAR explored effects of substitution in Zone A. For chemical accessibility, the dioxolane ring was replaced with isobutyl in many of the analogs (i.e., L-leucine benzyl ester was used in the 2 + 2 reaction). The affinity of the parent isobutyl analog, **18**, was 39 nM (see Fig. 6, below). Several alterations afforded a variety of azetidinones with a significant loss of V1a binding activity as represented in Figure 4. Similarly, a limited SAR at Zone B demonstrated that several modifications afforded derivatives with reduced V1a binding activity. Interestingly, replacing the phenyl with the 2-furyl substitution afforded a compound, **14**, with comparable activity, V1a IC_{50} = 2 nM (Fig. 5).

Zones C and D emerged as the most important points of structural modification. Removal of the Zone C substituent, as illustrated by the simple benzyl glycine derivative **5**, resulted in 10-fold loss of V1a activity, IC_{50} = 400 nM. Interestingly, acylation of **5** with base and pivaloyl chloride afforded **6** with significantly enhanced potency (V1a IC_{50} = 5 nM). Several Zone C modifications and attendant human IC_{50} values are shown in Figure 6.

In **1**, Zone D is occupied by the benzyl ester. The ester functionality was considered a potential metabolic weak point, so the first priority was to ascertain whether a more stable group such as amide could substitute for the ester linkage. As an intermediate, the trimethylsilyl ester derivative, **19**, was prepared. Despite having equivalent bulk and hydrophobicity to the benzyl group, the trimethylsilyl substitution resulted in reduced activity (V1a IC_{50} = 405 nM), indicating that the shape of the benzyl group was important. The trimethylsilyl ester, in turn, was transformed into the acid **20**, and subsequently coupled with benzylamine to afford the benzyl amide, **21** (V1a IC_{50} = 43 nM). Thus, the ester functionality of **1** could be converted to the corresponding amide, **21**, without loss of binding affinity (V1a IC_{50} = 45 nM vs V1a IC_{50} = 43 nM, respectively, see Fig. 7).

At this point, the next step for this project was to find a lead structure that combined high receptor affinity (IC_{50} < 10 nM) with useful brain levels (>10× the receptor affinity). Although **6** had good V1a binding affinity (IC_{50} = 5 nM), it provided minimal brain penetration in dogs treated orally with 10 mg/kg (dog brain concentration of **6**, 10 nM at 4 h). In an effort to find an amide substitution that would enhance oral absorption and CNS penetration, the L-leucyl platform was constructed (Fig. 8). Although not optimal for affinity, this platform was used as the basis for SAR exploration of Zone D because of its stability under conditions used for synthesis. The Zone D explorations had two objectives: to find the optimal substitution pattern for the benzylamide group, and to find other groups that would be compatible with high affinity, especially groups with charged functions

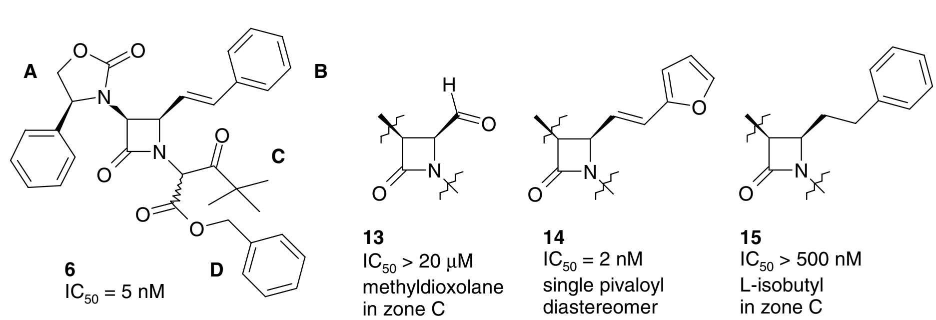

Figure 5. SAR overview of Zone B, 3 compounds prepared.

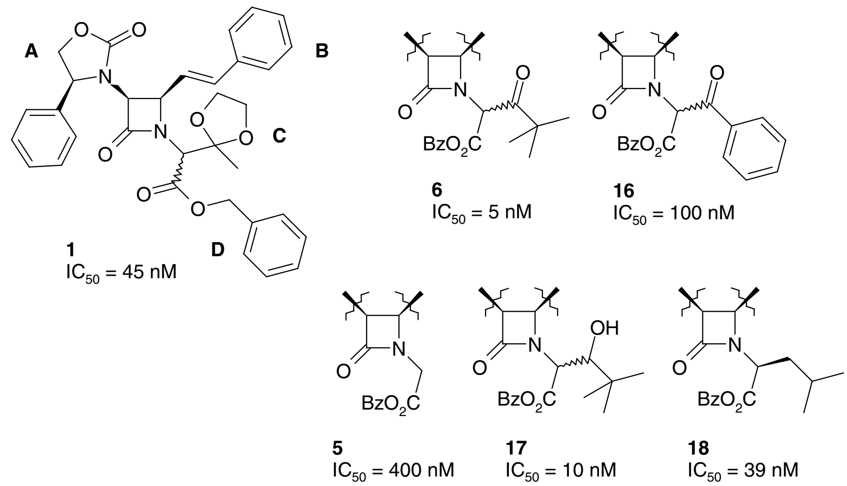

Figure 6. SAR overview of Zone C, 35 compounds prepared.

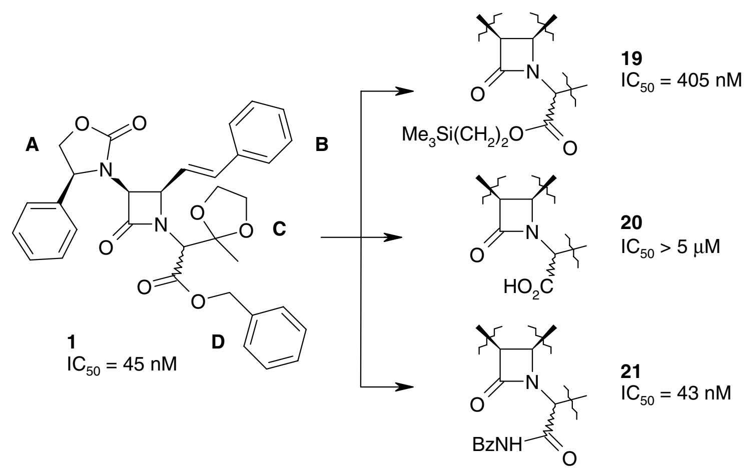

Figure 7. Acceptability of benzylamide in Zone D.

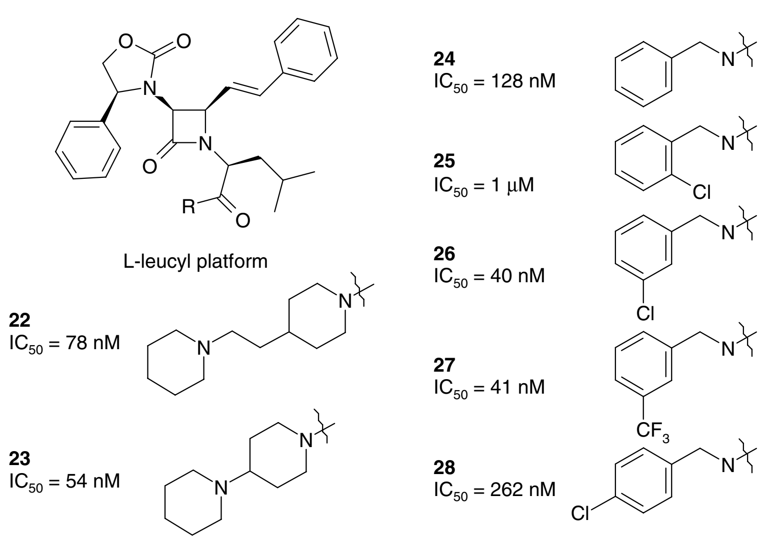

Figure 8. SAR overview of Zone D.

that would improve water solubility. Rapid solution-phase amide syntheses mediated by solid phase carbodiimide afforded over 50 amides,[22] some of which are illustrated in Figure 8.

A small substituent at the 3-position of the benzylamide (e.g., Cl or CF_3) was found to provide optimal affinity. Among groups other than benzyl, piperidylpiperidine and piperidyl-ethyl-piperidine provided relatively good

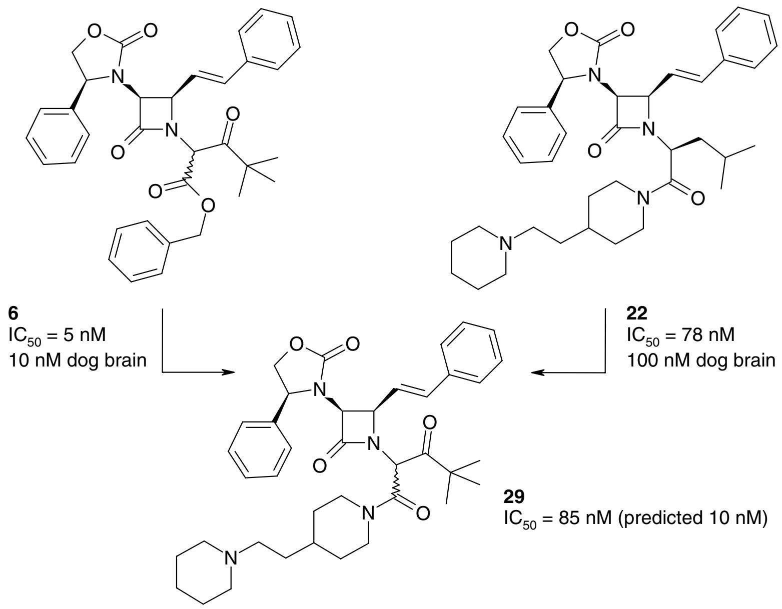

Figure 9. Non-additivity of the Zone C pivaloyl and Zone D piperidyl-ethyl-piperidine substitutions.

affinities. These groups would be positively charged at physiological pH, potentially leading to improved solubility. Interestingly, the piperidylpiperidine group was previously shown to provide optimal in vivo activity in an NK-1 clinical candidate.[23]

The piperidyl-ethyl-piperidine **22** was evaluated in dogs dosed orally at 10 mg/kg. Its brain level at 4 h post-administration was 100 nM, 10-fold better than **6** (see Fig. 9). Because the isobutyl substitution in Zone C was known to be suboptimal for V1a affinity, the corresponding compound with pivaloyl in Zone C was synthesized. Based on previous results, the pivaloyl group was expected to provide a roughly 8-fold boost in affinity, resulting in a predicted affinity of ~10 nM for the combination. Instead, affinity was 85 nM (Fig. 9).

In searching for an explanation of the non-additivity seen in **29**, it occurred to us that the binding mode of the molecule may have changed when benzyl was replaced with piperidyl-ethyl-piperidine. The two groups are after all completely different in shape and charge. With a proximally branched alkyl structure, the piperidyl-ethyl-piperidine group actually bears more resemblance to a typical Zone C substituent, such as methyldioxolane, pivaloyl, or isobutyl. We conjectured that the piperidyl-ethyl-piperidine bound into the Zone C pocket of the receptor, forcing the pivaloyl group into the free aqueous phase or into an unfavorable interaction with the Zone D pocket of the receptor. By this logic, reintroducing the benzylamide group in place of the pivaloyl should reoptimize binding in the Zone D pocket, creating a large boost in affinity. At this point, the vasopressin project was deprioritized, so confirmation of this hypothesis was put on hold pending completion of a successful out-licensing campaign.

After a four-year search for a partner, the program was reconstituted as a joint venture with Serenix Pharmaceuticals (later renamed Azevan), a start-up company created for this purpose. The initial strategy was to construct a scaffold with aminomalonic acid replacing L-leucine as depicted in Figure 10. If the piperidyl-ethyl-piperidine binds into Zone C according to the previous hypothesis, the binding pockets in Zones C and D should each tolerate a side chain anchored by an amide coupling, allowing the piperidyl-ethyl-piperidinamide and benzylamide to be present simultaneously. With the correct stereochemistry, each group should be able to bind to its preferred pocket. The relevant aminomalonate platform was synthesized as illustrated in Scheme 2. Gratifyingly, **33** showed a dramatic enhancement of human V1a binding affinity (V1a K_i = 1.17 nM, Fig. 11).

Even though there was significant improvement in binding affinity in the aminomalonyl platform azetidinones (Fig. 11), the compounds could only be obtained as diastereomeric mixtures, as a consequence of planarization of the malonate methine on dissociation of its acidic hydrogen. Consequently the L-aspartyl platform was prepared in the hope that this would retain the V1a binding affinity while obviating the issue of the labile methine hydrogen and the attendant diastereomeric mixture. These synthetic transformations are illustrated in Scheme 3. The most potent compound synthesized, **37**, had a V1a affinity comparable to that of **33** from the aminomalonyl platform (Fig. 12).

Theorizing that the D-aspartyl platform would be more resistant to in vivo enzymatic hydrolysis, we prepared the platform with a D-aspartyl group in Zones C and D (see Scheme 4). Although in general the D-platforms tended to be less active than the L-platforms (see the D-glutamyl platform, below), this was less pronounced for the D-aspartyl platform. In the case of **41** (V1a K_i 1.49 nM, Fig. 13), affinity of the D-aspartyl compound was actually slightly better than that of the corresponding L-aspartyl analog (**42**, V1a K_i = 1.89 nM). It is

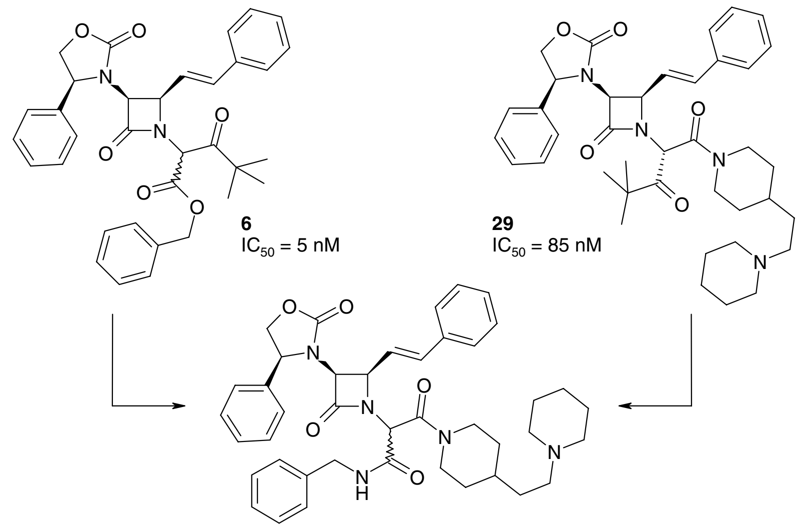

Figure 10. Rationale for aminomalonate platform.

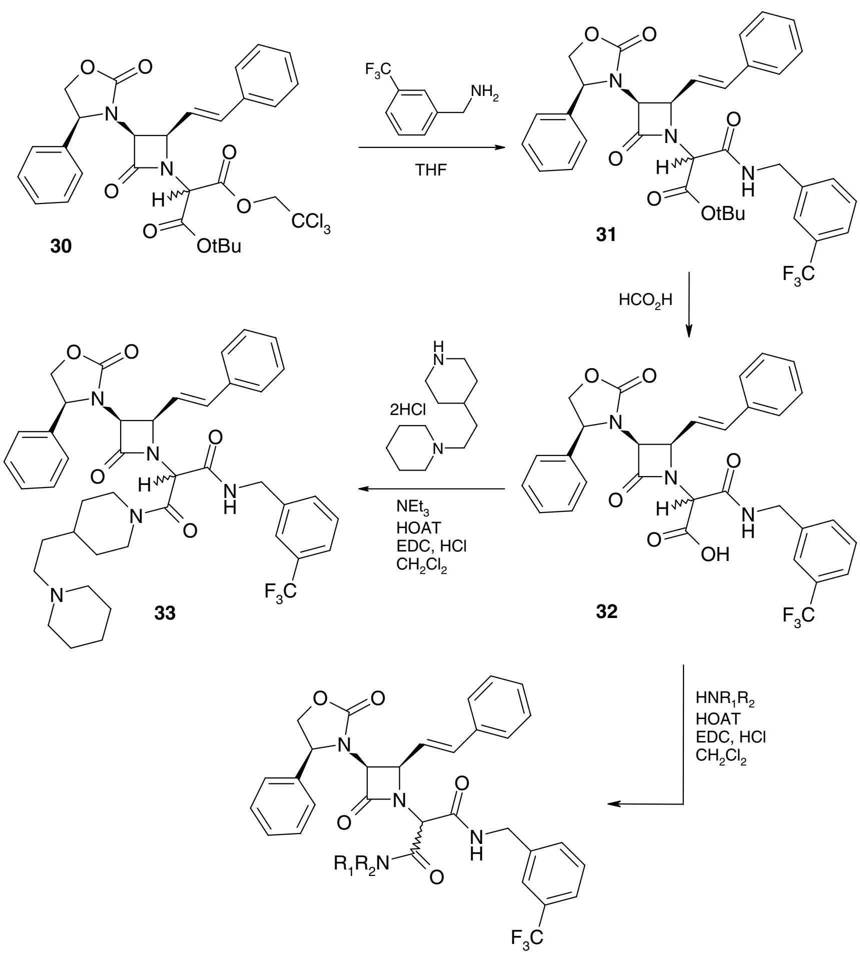

Scheme 2. Synthesis of **33** and analogs.

possible that the piperidylpiperidine side-chain may be able to adapt its conformation to match the receptor pocket in a unique way—a possibility that may also explain its superior pharmacokinetic properties in this series (vide infra) and the NK-1 series cited previously.[23]

The same reasons that led to the investigation of the L- and D-aspartyl platforms also resulted in the preparation of a range of compounds derived from L- and D-glutamic acids. The syntheses of these L- and D-glutamyl platforms are also illustrated in Schemes 3–5. The

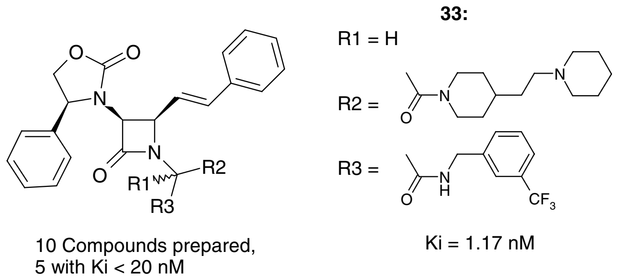

Figure 11. D,L-Aminomalonyl platform and attendant V1a affinity.

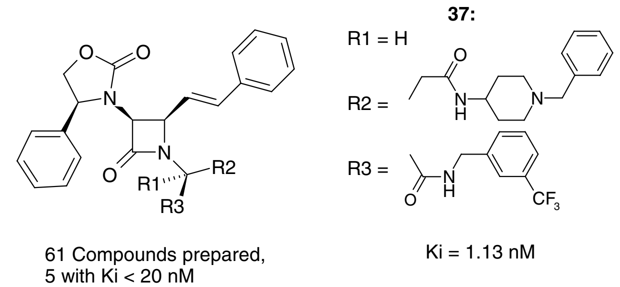

Figure 12. L-Aspartyl platform and attendant V1a affinity.

corresponding V1a binding affinities are shown (see Figs. 14 and 15). For these two series, the most active compounds were found to be L-glutamate analogs, with the D-glutamate versions being typically about 20-fold less active.

It is of interest that the highest affinity in the glutamyl platform was seen with the 4-cyclohexylpiperazine side chain, which is identical to the piperidylpiperidine side chain that gave optimal activity in the aspartyl platform, except that the basic amino group has been moved one bond closer, offsetting the additional methylene in the glutamyl moiety. In both of these examples, as well as in **37**, the positively charged group is 8 bonds away from the azetidine N. Thus, it appears that optimal activity requires a positively charged group at a fixed distance from the azetidinone core. It is possible that the basic nitrogen binds to the same site as the guanidinium of arginine–vasopressin.

Five of the compounds with $K_i < 10$ nM[24] were tested for plasma and brain levels in rats after oral dosing (20 mg/kg). Azetidinone **22** was used as a comparator. In this screening experiment, three compounds were dosed per animal, and plasma and brain levels were measured by LC/MS. Compound **41** showed the highest levels in both plasma and brain; however, several-fold lower levels were seen in follow-up experiments where

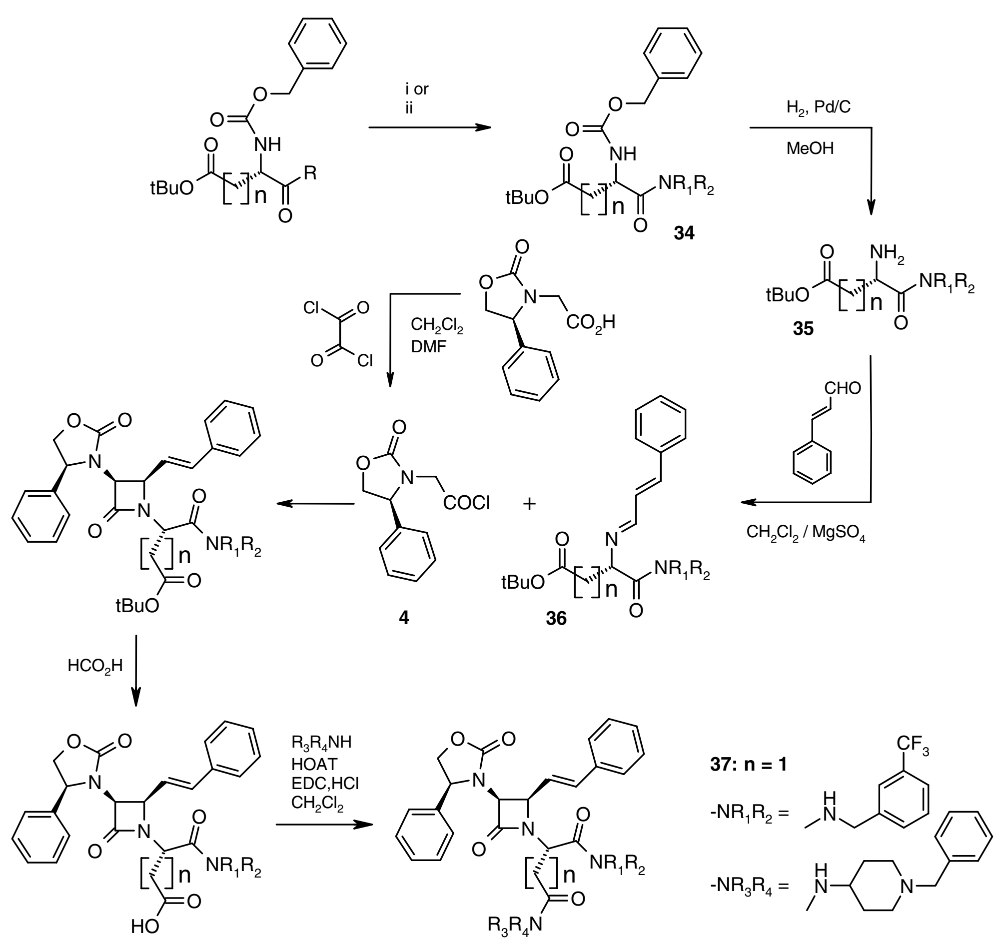

Scheme 3. Syntheses of L-aspartic and L-glutamic acid derivatives. R = –OSu. Reagents: (i) HNR_1R_2/THF; R = –OH, (ii) HNR_1R_2/HOBT/EDC, HCl/CH_2Cl_2.

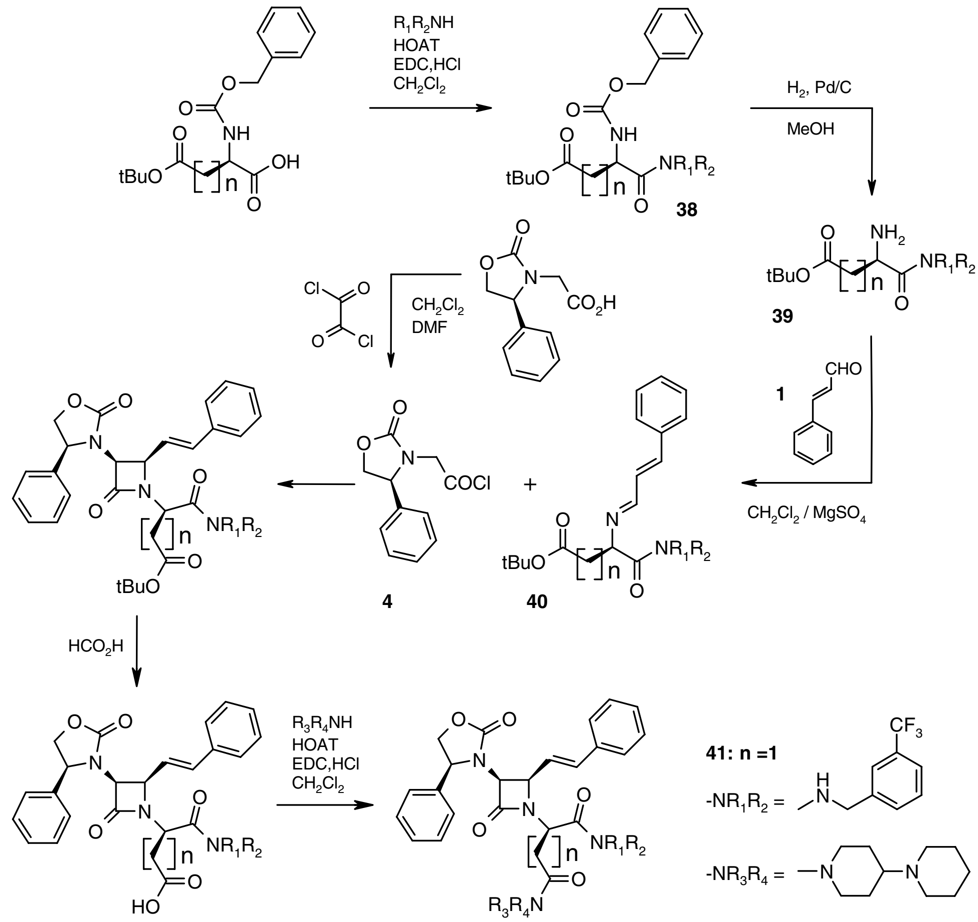

Scheme 4. Syntheses of D-aspartic and D-glutamic acid derivatives.

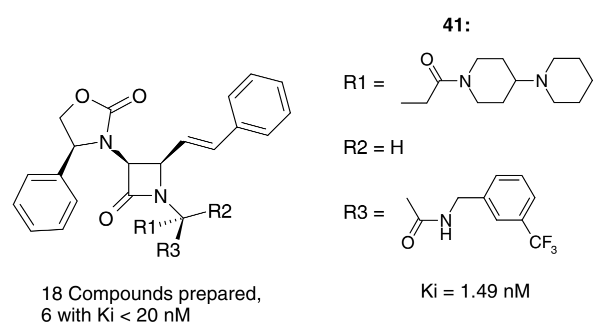

Figure 13. D-Aspartyl platform and attendant V1a affinity.

41 was dosed alone, suggesting that the initial higher levels were due in part to co-dosing with **22**. These results (plasma C_{max} 50–80 ng/ml in two separate experiments) were considered encouraging but fell somewhat short of expectations for a clinical candidate.

Theorizing that facile enzymatic cleavage of the benzylamide bond in Zone D reduced levels of **41**, we prepared **50** (**SRX246**) and **51** (**SRX251**) (see Fig. 16 for structures and Scheme 4 for synthetic pathway). It was hoped that these molecules, the (*R*)-α-methylbenzyl and the *N*-methyl analogs of **41**, respectively, would be more stable to enzymatic hydrolysis due to steric hindrance near the amide bond. Fortuitously, **50** and **51** proved to possess even higher in vitro V1a affinity than **41.** Compound **52**, the (*S*)-α-methylbenzyl diastereomer of **50**, was 600-fold less potent (V1a K_i = 179 nM). Interestingly, **53**, the trifluoromethyl analog of **50,** had reduced V1a binding affinity (see Fig. 16), suggesting that the α-methyl substitution shifted the binding mode of the adjacent phenyl ring. Azetidinone **54**, the *N*-methyl derivative of **50**, likewise had poor activity (V1a K_i = 9.8 nM), indicating that the *N*-methyl and α-methyl modifications also were incompatible.

Plasma levels for **50** and **51** were roughly double those of **41**, to some degree confirming the original motivation for the construction of these two compounds. C_{max} values were 100 ng/ml and 160 ng/ml, respectively, compared to 50–80 ng/ml for **41** (Fig. 17). Plasma T_{max} values for **50** and **51** were 4 h. Plasma $T_{1/2}$ values for **50** and **51** were 2.5 h and 4 h, respectively. The brain levels of **50** and **51** exceeded their K_i values by approximately 100-fold; brain C_{max} values of **50** and **51** were 20 ng/ml and 48 ng/ml, respectively, equivalent to 28 nM and 62 nM. Brain $T_{1/2}$ values of ~6 h for both compounds suggest the possibility of once-a-day dosing.

The binding affinity of all the reported compounds to other members of the vasopressin receptor family was also tested using cell lines that expressed human V1b and V2. The methods for human V1b and V2 binding assay are similar to that for V1a screening, namely the

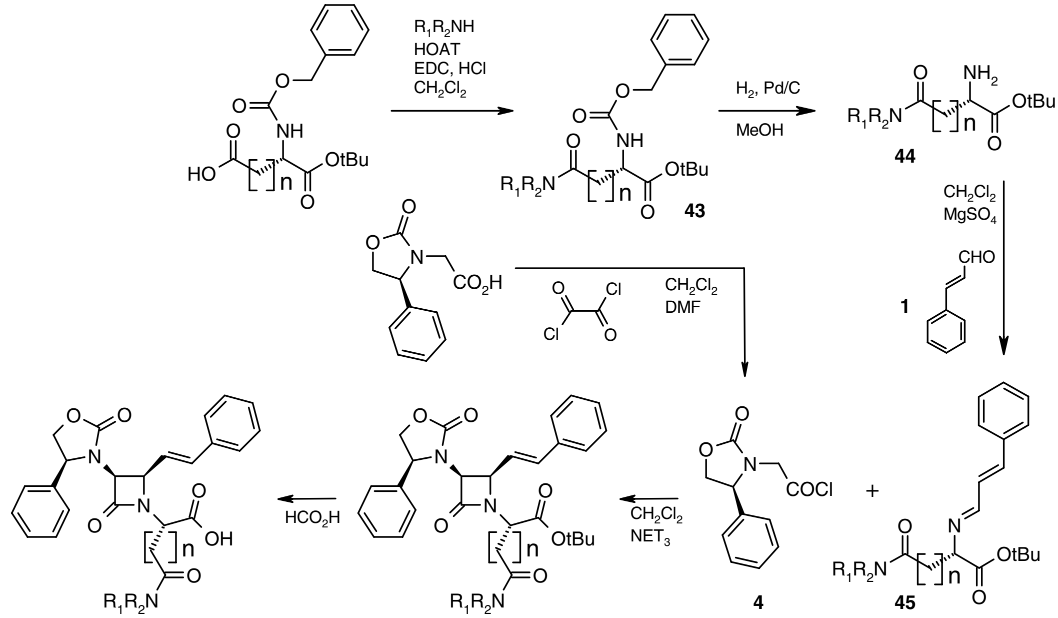

Scheme 5. Synthesis of additional L-glutamic acid derivatives.

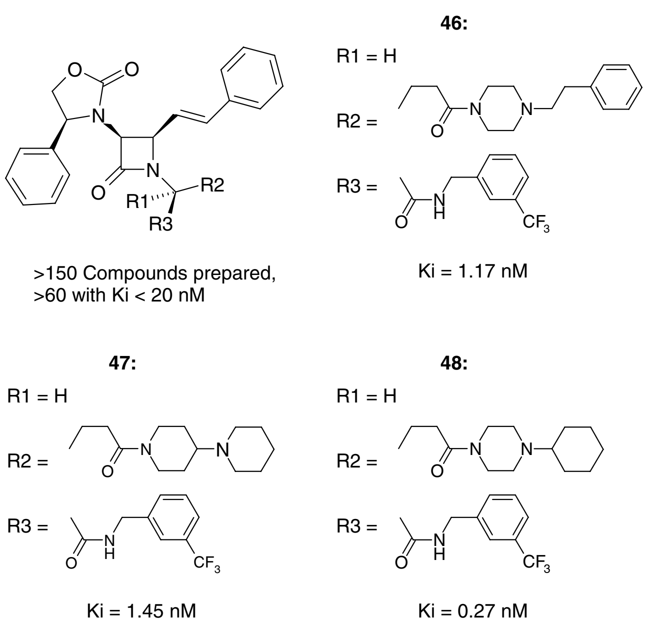

Figure 14. L-Glutamyl platform and attendant V1a affinity.

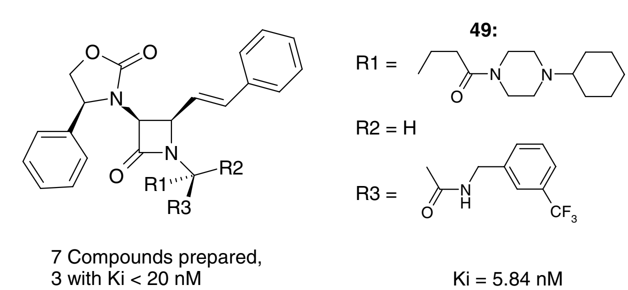

Figure 15. D-Glutamyl platform and attendant V1a affinity.

whole cell-based competitive binding assay, which is described in Section 4. The IC_{50} values of most Azevan compounds proved to be greater than 1 μM or 10 μM for both the V1b and V2 human receptor cell lines.

3. Conclusions

A novel series of vasopressin V1a antagonists has been designed from the unique monocyclic azetidinone platform. Subnanomolar affinities at the human V1a receptor have been achieved. On oral dosing, two members of the series, **50** (**SRX246**) and **51** (**SRX251**), reached brain levels ~100 times their in vitro receptor affinities. The candidate molecules are being further developed for human clinical evaluation.

4. Experimental

4.1. Chemistry

The early experimental work that was initially performed at Eli Lilly (preparation and characterization of LY307174, etc.) is described in Ref. 22.

4.1.1. (4(*S*)-Phenyloxazolidin-2-on-3-yl)acetyl chloride (4). This material was not produced in one batch but rather prepared as required for each 'chiral Staudinger 2 + 2 cycloaddition reaction.' Typically, a solution of 1 g (4.52 mmol) of (4(*S*)-phenyloxazolidin-2-on-3-yl)acetic acid (Evans, U.S. Patent No. 4,665,171) and 0.51 mL (5.88 mmol) of oxalyl chloride in 150 mL of dichloromethane was treated with a catalytic amount of anhydrous dimethylformamide (85 μL/mequiv of acetic acid derivative) resulting in vigorous gas evolution. After 45 min, all gas evolution had ceased

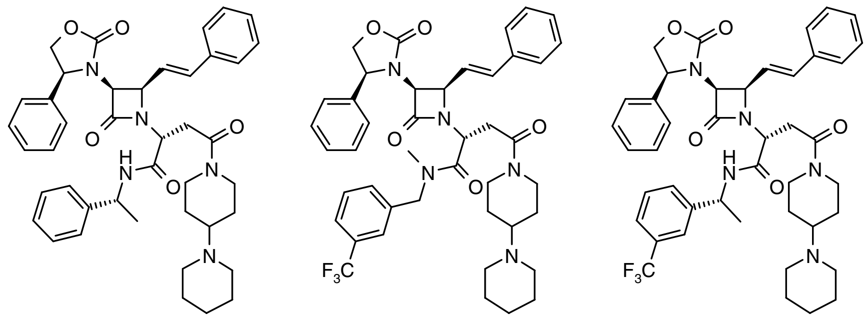

50, K_i = 0.3 nM **51,** K_i = 0.66 nM **53,** K_i = 1.27 nM

Figure 16. Structures and human V1a binding affinities of **50**, **51**, and **53**.

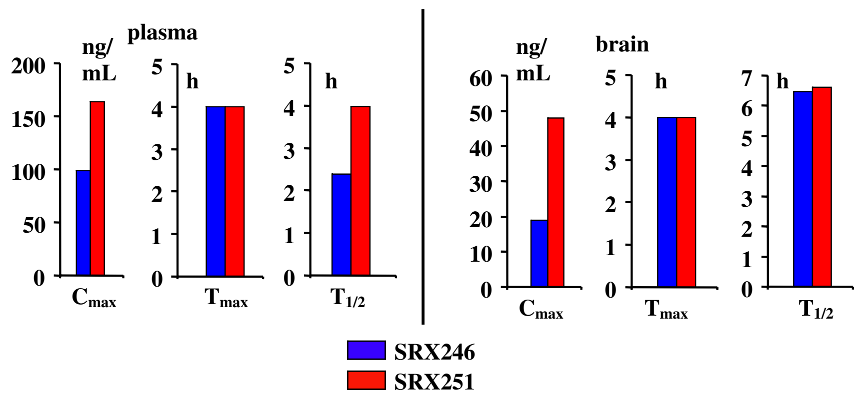

Figure 17. Oral pharmacokinetics of **SRX246** and **SRX251** in rats.

and the reaction mixture was concentrated under reduced pressure to provide the title compound as an off-white solid after drying for 2 h under vacuum. Compound **4** was used without purification for the 'chiral Staudinger [2 + 2] cycloaddition reaction.'

4.1.2. General procedure for an amide formation from an activated ester derivative

4.1.2.1. *N*-Benzyloxycarbonyl-L-aspartic acid β-*tert*-butyl ester α-(3-trifluoromethyl)benzylamide (34a, 34 with HNR_1R_2 = 3-(trifluoromethyl)benzylamine and *n* = 1). A solution of *N*-benzyloxycarbonyl-L-aspartic acid β-*tert*-butyl ester α-*N*-hydroxysuccinimide ester (1.95 g, 4.64 mmol, Advanced ChemTech) in 20 mL of dry tetrahydrofuran was treated with 0.68 mL (4.74 mmol) of 3-(trifluoromethyl)benzylamine. Upon completion of the reaction as monitored by TLC (60:40 hexanes/ethyl acetate), the solvent was evaporated, and the resulting oil was partitioned between dichloromethane and a saturated aqueous solution of sodium bicarbonate. The organic layer was dried over magnesium sulfate, filtered, and evaporated to give 2.23 g (quantitative yield) of the title compound as a white solid; ^{1}H NMR ($CDCl_3$) δ 1.39 (s, 9H); 2.61 (dd, *J* = 6.5 Hz, *J* = 17.2 Hz, 1H); 2.98 (dd, *J* = 3.7 Hz, *J* = 17.0 Hz, 1H); 4.41 (dd, *J* = 5.9 Hz, *J* = 15.3 Hz, 1H); 4.50–4.57 (m, 2H); 5.15 (s, 2H); 5.96–5.99 (m, 1H); 6.95 (s, 1H); 7.29–7.34 (m, 5H); 7.39–7.43 (m, 2H); 7.48–7.52 (m, 2H).

The following compounds were obtained according to this procedure:

4.1.2.2. *N*-Benzyloxycarbonyl-L-aspartic acid β-*tert*-butyl ester α-[4-(2-phenylethyl)]piperazinamide (34b, 34 with HNR_1R_2 = 4-(phenylethyl)piperazine and *n* = 1). Use of *N*-benzyloxycarbonyl-L-aspartic acid β-*tert*-butyl ester α-*N*-hydroxysuccinimide ester (5.0 g, 12 mmol, Advanced ChemTech) and 4-(phenylethyl)piperazine 2.27 mL (11.9 mmol) gave 5.89 g (quantitative yield) of **34b** as a white solid; ^{1}H NMR ($CDCl_3$) δ 1.40 (s, 9H); 2.45–2.80 (m, 10H); 3.50–3.80 (m, 4H); 4.87–4.91 (m, 1H); 5.08 (s, 2H); 5.62–5.66 (m, 1H); 7.17–7.33 (m, 10H).

4.1.2.3. *N*-Benzyloxycarbonyl-L-glutamic acid γ-*tert*-butyl ester α-(3-trifluoromethyl)benzylamide (34c, 34 with HNR_1R_2 = 3-(trifluoromethyl)benzylamine and *n* = 2). Use of *N*-benzyloxycarbonyl-L-glutamic acid β-*tert*-butyl ester α-*N*-hydroxysuccinimide ester (4.83 g, 11.1 mmol, Advanced ChemTech) and 3-(trifluoromethyl)benzylamine 1.63 mL (11.4 mmol) gave 5.41 g (98%) of **34c** as a white solid; ^{1}H NMR ($CDCl_3$) δ 1.40 (s, 9H); 1.88–1.99 (m, 1H); 2.03–2.13 (m, 1H); 2.23–2.33 (m, 1H); 2.38–2.47 (m, 1H); 4.19–4.25 (s, 1H); 4.46–4.48 (m, 2H); 5.05–5.08 (m, 2H); 5.67–5.72 (m, 1H); 7.27–7.34 (m, 5H); 7.39–7.43 (m, 2H); 7.48–7.52 (m, 2H).

4.1.3. General procedure for amide formation from a carboxylic acid

4.1.3.1. *N*-Benzyloxycarbonyl-D-aspartic acid β-*tert*-butyl ester α-(3-trifluoromethyl)benzylamide (38a, 38 with HNR_1R_2 = 3-(trifluoromethyl)benzylamine and *n* = 1). A solution of 1 g (2.93 mmol) of *N*-benzyloxycarbonyl-D-aspartic acid β-*tert*-butyl ester monohydrate

(Novabiochem) in 3–4 mL of dichloromethane was treated by sequential addition of 0.46 mL (3.21 mmol) of 3-(trifluoromethyl)benzylamine, 0.44 g (3.23 mmol) of 1-hydroxy-7-benzotriazole, and 0.62 g (3.23 mmol) of 1-[3-(dimethylamino)propyl]-3-ethylcarbodiimide hydrochloride. After at least 12 h at ambient temperature or until complete as determined by thin layer chromatography (95:5 dichloromethane/methanol eluent), the reaction mixture was washed sequentially with a saturated aqueous sodium bicarbonate solution and with distilled water. The organic layer was dried over magnesium sulfate, filtered, and evaporated to give 1.41 g (quantitative yield) of **38a** as a white solid; ^{1}H NMR ($CDCl_3$) δ 1.39 (s, 9H); 2.61 (dd, $J = 6.5$ Hz, $J = 17.2$ Hz, 1H); 2.98 (dd, $J = 4.2$ Hz, $J = 17.2$ Hz, 1H); 4.41 (dd, $J = 5.9$ Hz, $J = 15.3$ Hz, 1H); 4.50–4.57 (m, 2H); 5.10 (s, 2H); 5.96–6.01 (m, 1H); 6.91–7.00 (m, 1H); 7.30–7.36 (m, 5H); 7.39–7.43 (m, 2H); 7.48–7.52 (m, 2H).

The following compounds were obtained according to this procedure:

4.1.3.2. *N*-Benzyloxycarbonyl-D-aspartic acid β-*tert*-butyl ester α-(2-fluoro-3-trifluoromethyl)benzylamide (38b, 38 with HNR_1R_2 = (2-fluoro-3-trifluoromethyl)benzylamine and *n* = 1). Use of *N*-benzyloxycarbonyl-D-aspartic acid β-*tert*-butyl ester monohydrate (Novabiochem) (0.25 g, 0.73 mmol) and 0.12 mL of (2-fluoro-3-trifluoromethyl)benzylamine gave 0.365 g (quantitative yield) of **38b** as a white solid; ^{1}H NMR ($CDCl_3$) δ 1.38 (s, 9H); 2.59 (dd, $J = 6.5$ Hz, $J = 17.0$ Hz, 1H); 2.95 (dd, $J = 4.3$ Hz, $J = 17.0$ Hz, 1H); 4.46–4.56 (m, 3H); 5.11 (s, 2H); 5.94–5.96 (m, 1H); 7.15 (t, $J = 8.0$ Hz, 1H); 7.30–7.36 (m, 5H); 7.47–7.52 (m, 2H).

4.1.3.3. *N*-Benzyloxycarbonyl-D-aspartic acid β-*tert*-butyl ester α-[(*S*)-α-methylbenzyl]amide (38c, 38 with HNR_1R_2 = (*S*)-α- methylbenzylamine and *n* = 1). Use of *N*-benzyloxycarbonyl-D-aspartic acid β-*tert*-butyl ester monohydrate (Novabiochem) (0.25 g, 0.73 mmol) and 0.094 mL of (*S*)-α-methylbenzylamine gave 0.281 g (90%) of **38c** as a white solid; ^{1}H NMR ($CDCl_3$) δ 1.41 (s, 9H); 1.44 (d, $J = 7.0$ Hz, 3H); 2.61 (dd, $J = 7.0$ Hz, $J = 17.0$ Hz, 1H); 2.93 (dd, $J = 4.0$ Hz, $J = 17.5$ Hz, 1H); 4.50–4.54 (m, 1H); 5.04–5.14 (m, 3H); 5.94–5.96 (m, 1H); 6.76–6.80 (m, 1H); 7.21–7.37 (m, 10H).

4.1.3.4. *N*-Benzyloxycarbonyl-D-aspartic acid β-*tert*-butyl ester α-[(*R*)-α-methylbenzyl]amide (38d, 38 with HNR_1R_2 = (*R*)-α-methylbenzylamine and *n* = 1). Use of *N*-benzyloxycarbonyl-D-aspartic acid β-*tert*-butyl ester monohydrate (Novabiochem) (0.25 g, 0.73 mmol) and 0.094 mL of (*R*)-α-methylbenzylamine gave 0.281 g (90%) of **38d** as a white solid; ^{1}H NMR ($CDCl_3$) δ 1.38 (s, 9H); 1.43 (d, $J = 6.9$ Hz, 3H); 2.54 (dd, $J = 7.3$ Hz, $J = 17.2$ Hz, 1H); 2.87 (dd, $J = 4.1$ Hz, $J = 17.2$ Hz, 1H); 4.46–4.50 (m, 1H); 4.99–5.15 (m, 3H); 5.92–5.96 (m, 1H); 6.78–6.82 (m, 1H); 7.21–7.33 (m, 10H). ^{13}C NMR ($CDCl_3$) δ 21.99, 27.95, 37.58, 50.03, 50.92, 67.13, 81.87, 125.95, 126.72, 128.05, 128.21, 128.52, 128.58, 129.07, 136.08, 142.86, 155.93, 169.34, 171.31.

4.1.3.5. *N*-Benzyloxycarbonyl-D-aspartic acid γ-*tert*-butyl ester α-[*N*-methyl-*N*-(3-trifluoromethylbenzyl)]amide (38e, 38 with HNR_1R_2 = *N*-methyl-*N*-(3-trifluoromethylbenzyl)amine and *n* = 1). Use of *N*-benzyloxycarbonyl-D-aspartic acid γ-*tert*-butyl ester (0.303 g, 0.89 mmol, Novabiochem) and 0.168 g (0.89 mmol,) of *N*-methyl-*N*-(3-trifluoromethylbenzyl)amine gave 0.287 g (65%) of **38e** as a white solid; ^{1}H NMR ($CDCl_3$) δ 1.40 (s, 9H); 2.55 (dd, $J = 5.8$ Hz, $J = 15.8$ Hz, 1H); 2.81 (dd, $J = 7.8$ Hz, $J = 15.8$ Hz, 1H); 4.10 (s, 3H); 4.25 (d, $J = 15.0$ Hz, 1H); 4.80 (d, $J = 15.5$ Hz, 1H); 5.01–5.13 (m, 3H); 5.52–5.55 (m, 1H); 7.25–7.52 (m, 10H).

4.1.3.6. *N*-Benzyloxycarbonyl-D-aspartic acid β-*tert*-butyl ester α-[(*S*)-1-(3-trifluoromethylphenyl)ethyl]amide (38f, 38 with HNR_1R_2 = (*S*)-1-(3-trifluoromethylphenyl)ethylamine and *n* = 1). Use of *N*-benzyloxycarbonyl-D-aspartic acid β-*tert*-butyl ester monohydrate (Novabiochem) (84 mg, 0.25 mmol) and 47 mg of (*S*)-1-(3-trifluoromethylphenyl)ethylamine gave 122 mg (quantitative yield) of **38f** as a white solid; ^{1}H NMR ($CDCl_3$) δ 1.38 (s, 9H); 1.43 (d, $J = 7.0$ Hz, 3H); 2.59 (dd, $J = 6.7$ Hz, $J = 17.3$ Hz, 1H); 2.93 (dd, $J = 4.1$ Hz, $J = 17.3$ Hz, 1H); 4.49–4.53 (m, 1H); 5.05–5.28 (m, 3H); 5.91–5.95 (m, 1H); 6.84–6.87 (m, 1H); 7.29–7.52 (m, 9H).

4.1.3.7. *N*-Benzyloxycarbonyl-D-aspartic acid β-*tert*-butyl ester α-[(*R*)-1-(3-trifluoromethylphenyl)ethyl]amide (38g, 38 with HNR_1R_2 = (*R*)-1-(3-trifluoromethylphenyl)ethylamine and *n* = 1). Use of *N*-benzyloxycarbonyl-D-aspartic acid β-*tert*-butyl ester monohydrate (Novabiochem) (150 mg, 0.44 mmol) and 83 mg of (*R*)-1-(3-trifluoromethylphenyl)ethylamine gave 217 mg (quantitative yield) of **38g** as a white solid; ^{1}H NMR ($CDCl_3$) δ 1.38 (s, 9H); 1.43 (d, $J = 7.0$ Hz, 3H); 2.54 (dd, $J = 7.4$ Hz, $J = 17.3$ Hz, 1H); 2.87 (dd, $J = 4.0$ Hz, $J = 17.3$ Hz, 1H); 4.47–4.51 (m, 1H); 5.01–5.16 (m, 3H); 5.92–5.96 (m, 1H); 6.90–6.94 (m, 1H); 7.26–7.49 (m, 9H).

4.1.3.8. *N*-Benzyloxycarbonyl-D-glutamic acid γ-*tert*-butyl ester α-(3-trifluoromethyl)benzylamide (38h, 38 with HNR_1R_2 = 3-(trifluoromethyl)benzylamine and *n* = 2). Use of *N*-benzyloxycarbonyl-D-glutamic acid γ-*tert*-butyl ester (1.14 g, 3.37 mmol) and 0.53 mL (3.70 mmol, Novabiochem) of 3-(trifluoromethyl)benzylamine gave 1.67 g (quantitative yield) of **38h** as a white solid; ^{1}H NMR ($CDCl_3$) δ 1.40 (s, 9H), 1.89–1.97 (m, 1H); 2.04–2.12 (m, 1H); 2.24–2.31 (m, 1H); 2.39–2.46 (m, 1H); 4.19–4.24 (s, 1H); 4.45–4.48 (m, 2H); 5.03–5.09 (m, 2H); 5.71–5.74 (m, 1H); 6.83–6.88 (m, 1H); 7.26–7.34 (m, 5H); 7.40–7.43 (m, 2H); 7.49–7.52 (m, 2H).^{13}C NMR ($CDCl_3$) δ 27.86, 27.99, 31.73, 54.51, 67.11, 81.19, 122.90, 124.22 (q, $^3J_{C-F}$, 4.0 Hz, 1C), 124.31 (q, $^3J_{C-F}$, 3.7 Hz, 1C), 125.06, 128.03, 128.22, 128.52, 129.17, 130.88, 130.98 (q, $^1J_{C-F}$, 32.3 Hz, CF_3), 136.07, 139.02, 171.43, 172.92.

4.1.3.9. *N*-Benzyloxycarbonyl-L-glutamic acid α-*tert*-butyl ester γ-(4-cyclohexyl)piperazinamide: (43a, 43 with HNR_1R_2 = 1-cyclohexylpiperazine and *n* = 2). Use of *N*-benzyloxycarbonyl-L-glutamic acid α-*tert*-butyl ester

(1.36 g, 4.03 mmol) and 0.746 g (4.43 mmol) of 1-cyclohexylpiperazine gave 1.93 g (98%) of **43a** as a white solid; ^{1}H NMR ($CDCl_3$) δ 1.02–1.12 (m, 5H); 1.43 (s, 9H), 1.60–1.64 (m, 1H); 1.80–1.93 (m, 5H); 2.18–2.52 (m, 8H); 3.38–3.60 (m, 4H); 4.20–4.24 (m, 1H); 5.03–5.13 (m, 2H); 5.53–5.57 (m, 1H); 7.28–7.34 (m, 5H).

4.1.4. General procedure for hydrogenation of a benzyloxycarbonyl amine

4.1.4.1. L-Aspartic acid β-*tert*-butyl ester α-(3-trifluoromethyl)benzylamide (35a, 35 with HNR_1R_2 = 3-(trifluoromethyl)benzylamine and *n* = 1). A suspension of 2.23 g (4.64 mmol) of *N*-benzyloxycarbonyl-L-aspartic acid β-*tert*-butyl ester α-(3-trifluoromethyl)benzylamide **34a** and palladium (5% wt. on activated carbon, 0.642 g) in 30 mL of methanol was held under an atmosphere of hydrogen until complete conversion as determined by thin layer chromatography (95:5 dichloromethane/methanol eluent). The reaction was filtered to remove the palladium over carbon and the filtrate was evaporated to give 1.52 g (96%) of **7a** as an off-white solid; ^{1}H NMR ($CDCl_3$) δ 1.42 (s, 9H); 2.26 (br s, 2H); 2.63–2.71 (m, 1H); 2.82–2.87 (m, 1H); 3.75–3.77 (m, 1H); 4.47–4.50 (m, 2H); 7.41–7.52 (m, 4H); 7.90 (br s, 1H).

The following compounds were obtained according to this procedure:

4.1.4.2. L-Aspartic acid β-*tert*-butyl ester α-[4-(2-phenylethyl)]piperazinamide (35b, 35 with HNR_1R_2 = 4-(phenylethyl)piperazine and *n* = 1). Use of *N*-benzyloxycarbonyl-L-aspartic acid β-*tert*-butyl ester α-[4-(2-phenylethyl)]piperazinamide (5.89 g, 11.9 mmol) **34b** gave 4.24 g (98%) of **35b** as an off-white solid; ^{1}H NMR ($CDCl_3$): δ 1.42 (s, 9H); 2.61–2.95 (m, 10H); 3.60–3.90 (m, 4H); 4.35–4.45 (m, 1H); 7.17–7.29 (m, 5H).

4.1.4.3. L-Glutamic acid γ-*tert*-butyl ester α-(3-trifluoromethyl)benzylamide (35c, 35 with HNR_1R_2 = 3-(trifluoromethyl)benzylamine and *n* = 2). Use of *N*-benzyloxycarbonyl-L-glutamic acid γ-*tert*-butyl ester α-(3-trifluoromethyl)benzylamide (5.41 g, 10.9 mmol) **34c** gave 3.94 g (quantitative yield) of **35c** as an off-white solid; ^{1}H NMR ($CDCl_3$): δ 1.41 (s, 9H); 1.73–1.89 (m, 3H); 2.05–2.16 (m, 1H); 2.32–2.38 (m, 2H); 3.47 (dd, J = 5.0 Hz, J = 7.5 Hz, 1H); 4.47–4.49 (m, 2H); 7.36–7.54 (m, 4H); 7.69–7.77 (m, 1H).

4.1.4.4. D-Aspartic acid β-*tert*-butyl ester α-(3-trifluoromethyl)benzylamide (39a, 39 with HNR_1R_2 = 3-(trifluoromethyl)benzylamine and *n* = 1). Use of *N*-benzyloxycarbonyl-D-aspartic acid β-*tert*-butyl ester α-(3-trifluoromethyl)benzylamide (1.41 g, 2.93 mmol) **38a** gave 0.973 g (96%) of **39a** as an off-white solid; ^{1}H NMR ($CDCl_3$): δ 1.42 (s, 9H); 2.21 (br s, 2H); 2.67 (dd, J = 7.1 Hz, J = 16.8 Hz, 1H); 2.84 (dd, J = 3.6 Hz, J = 16.7 Hz, 1H); 3.73–3.77 (m, 1H); 4.47–4.50 (m, 2H); 7.41–7.52 (m, 4H); 7.83–7.87 (m, 1H).

4.1.4.5. D-Aspartic acid β-*tert*-butyl ester α-(2-fluoro-3-trifluoromethyl)benzylamide (39b, 39 with HNR_1R_2 = (2-fluoro-3-trifluoromethyl)benzylamine and *n* = 1). Use of *N*-benzyloxycarbonyl-D-aspartic acid β-*tert*-butyl ester α-(2-fluoro-3-trifluoromethyl)benzylamide **38b** (0.36 g, 0.72 mmol) gave 0.256 g (92%) of **39b** as an off-white solid; ^{1}H NMR ($CDCl_3$) δ 1.39 (s, 9H); 2.50 (br s, 2H); 2.74 (dd, J = 7.0 Hz, J = 16.5 Hz, 1H); 2.86 (dd, J = 4.8 Hz, J = 16.8 Hz, 1H); 3.89 (br s, 2H); 4.47–4.57 (m, 2H); 7.16 (t, J = 7.8 Hz, 1H); 7.48 (t, J = 7.3 Hz, 1H); 7.56 (t, J = 7.3 Hz, 1H); 7.97–8.02 (m, 1H).

4.1.4.6. D-Aspartic acid β-*tert*-butyl ester α-[(*S*)-α-methyl]benzylamide (39c, 39 with HNR_1R_2 = (*S*)-α-methylbenzylamine and *n* = 1). Use of *N*-benzyloxycarbonyl-D-aspartic acid β-*tert*-butyl ester α-[(*S*)-α-methylbenzyl]amide (0.275 g, 0.65 mmol) **38c** gave 0.17 g (90%) of **39c** as an off-white solid; ^{1}H NMR ($CDCl_3$) δ 1.40 (s, 9H); 1.47 (d, J = 6.9 Hz, 3H); 1.98 (br s, 2H); 2.49 (dd, J = 7.9 Hz, J = 17.7 Hz, 1H); 2.83 (dd, J = 3.6 Hz, J = 16.7 Hz, 1H); 3.69 (br s, 1H); 4.99–5.10 (m, 1H); 7.19–7.33 (m, 5H); 7.65–7.68 (m, 1H).

4.1.4.7. D-Aspartic acid β-*tert*-butyl ester α-[(*R*)-α-methylbenzyl]amide (39d, 39 with HNR_1R_2 = (*R*)-α-methylbenzylamine and *n* = 1). Use of *N*-benzyloxycarbonyl-D-aspartic acid β-*tert*-butyl ester α-[(*R*)-α-methylbenzyl]amide (0.273 g, 0.64 mmol) **38d** gave 0.187 g (quantitative yield) of **39d** as an off-white solid; ^{1}H NMR (CD_3OD) δ 1.40 (s, 9H); 1.46 (d, J = 7.0 Hz, 3H); 2.49 (dd, J = 7.0 Hz, J = 16.5 Hz, 1H); 2.61 (dd, J = 5.5 Hz, J = 16.0 Hz, 1H); 3.62 (dd, J = 6.0 Hz, J = 7.0 Hz, 1H); 4.98 (dd, J = 7.0 Hz, J = 14.0 Hz, 1H); 7.20–7.23 (m, 1H); 7.27–7.34 (m, 4H); ^{13}C NMR (CD_3OD) δ 22.45, 28.31, 41.38, 50.17, 52.92, 82.17, 127.13, 128.09, 129.53, 144.96, 172.14, 175.11.

4.1.4.8. D-Aspartic acid β-*tert*-butyl ester α-[*N*-methyl-*N*-(3-trifluoromethylbenzyl)]amide (39e, 39 with HNR_1R_2 = *N*-methyl-*N*-(3-trifluoromethylbenzyl)amine and *n* = 1). Use of *N*-benzyloxycarbonyl-D-aspartic acid β-*tert*-butyl ester α-[*N*-methyl-*N*-(3-trifluoromethylbenzyl)]amide **38e** (0.282 g, 0.57 mmol) gave 0.195 g (95%) of **39e** as an off-white solid. Compound **10e** exhibited a ^{1}H NMR spectrum consistent with the assigned structure.

4.1.4.9. D-Aspartic acid β-*tert*-butyl ester α-[(*S*)-1-(3-trifluoromethylphenyl)ethyl]amide (39f, 39 with HNR_1R_2 = (*S*)-1-(3-trifluoromethylphenyl)ethylamine and *n* = 1). Use of *N*-benzyloxycarbonyl-D-aspartic acid β-*tert*-butyl ester α-[(*S*)-1-(3-trifluoromethylphenyl)ethyl]amide **38f** (120 mg, 0.24 mmol) gave 80 mg (91%) of **39f** as an off-white solid; ^{1}H NMR (MeOH-d_4) δ 1.42 (s, 9H); 1.48 (d, J = 7.1 Hz, 3H); 2.58 (dd, J = 7.0 Hz, J = 16.8 Hz, 1H); 2.69 (dd, J = 5.8 Hz, J = 16.8 Hz, 1H); 3.77–3.89 (m, 1H); 5.03–5.09 (m, 1H); 7.48–7.65 (m, 4H).

4.1.4.10. D-Aspartic acid β-*tert*-butyl ester α-[(*R*)-1-(3-trifluoromethylphenyl)ethyl]amide (39g, 39 with HNR_1R_2 = (*R*)-1-(3-trifluoromethylphenyl)ethylamine and *n* = 1). Use of *N*-benzyloxycarbonyl-D-aspartic acid β-*tert*-butyl ester α-[(*R*)-1-(3-trifluoromethylphenyl)ethyl]amide **38g** (217 mg, 0.44 mmol) gave 157 mg (quantitative yield) of **39g** as an off-white solid; ^{1}H NMR

(MeOH-d_4) δ 1.39 (s, 9H); 1.49 (d, J = 7.1 Hz, 3H); 2.55 (dd, J = 6.6 Hz, J = 16.4 Hz, 1H); 2.63 (dd, J = 5.7 Hz, J = 16.4 Hz, 1H); 3.60–3.64 (m, 1H); 5.00–5.08 (m, 1H); 7.47–7.67 (m, 4H).

4.1.4.11. D-Glutamic acid γ-*tert*-butyl ester α-(3-trifluoromethyl)benzylamide (39h, 39 with HNR_1R_2 = 3-(trifluoromethyl)benzylamine and *n* = 2). Use of *N*-benzyloxycarbonyl-D-glutamic acid γ-*tert*-butyl ester α-(3-trifluoromethyl)benzylamide (1.667 g, 3.37 mmol) **38h** gave 1.15 g (94%) of **39h** as an off-white solid; ^{1}H NMR ($CDCl_3$) δ 1.41 (s, 9H); 1.80–2.20 (m, 4H); 2.31–2.40 (m, 2H); 3.51–3.59 (m, 1H); 4.47–4.49 (m, 2H); 7.39–7.52 (m, 4H); 7.71–7.79 (m, 1H).

4.1.4.12. L-Glutamic acid α-*tert*-butyl ester γ-(4-cyclohexyl)piperazinamide (44a, 44 with HNR_1R_2 = 1-cyclohexylpiperazine and *n* = 2). Use of *N*-benzyloxycarbonyl-L-glutamic acid α-*tert*-butyl ester γ-(4-cyclohexyl)piperazinamide (1.93 g, 3.96 mmol) **43a** gave 1.30 g (93%) of **44a** as an off-white solid; ^{1}H NMR ($CDCl_3$) δ 1.02–1.25 (m, 5H); 1.41 (s, 9H); 1.45–1.50 (m, 1H); 1.56–1.60 (m, 1H); 1.69–1.80 (m, 6H); 3.30 (dd, J = 4.8 Hz, J = 8.5 Hz, 1H); 3.44 (t, J = 9.9 Hz, 2H); 3.56 (t, J = 9.9 Hz, 2H).

4.1.5. General procedure for formation of a 2-azetidinone from an imine and an acetyl chloride

4.1.5.1. Step 1. General procedure for formation of an imine from an amino acid derivative. A solution of 1 equiv of an α-amino acid ester or amide (such as **35**, **39** or **44**) in dichloromethane was treated sequentially with 1 equiv of an appropriate aldehyde (such as *t*-cinnamaldehyde), and a desiccating agent, such as magnesium sulfate or silica gel, in the amount of about 2 g of desiccating agent per gram of starting α-amino acid ester or amide. The reaction mixture was stirred at ambient temperature until all of the reactants were consumed as measured by thin layer chromatography (CH_2Cl_2 95%/MeOH 5%). When complete, the reaction mixture was then filtered, the filter cake was washed with dichloromethane, and the filtrate concentrated under reduced pressure to provide the desired imine that was used as it is in the subsequent step.

4.1.5.2. Step 2. General procedure for the [2 + 2] cycloaddition of an imine and an acetyl chloride. A dichloromethane solution of the imine (such as **36**, **40**, or **45**) (10 mL dichloromethane/1 g imine) was cooled to 0 °C. To this cooled solution was added 1.5 equiv of an appropriate amine, typically triethylamine, followed by the dropwise addition of a dichloromethane solution of 1.1 equiv of an appropriate acetyl chloride (such as **4**) (10 mL of dichloromethane/1 g appropriate acetyl chloride). The reaction mixture was allowed to warm to ambient temperature over 1 h and was then quenched by the addition of a saturated aqueous solution of ammonium chloride. The resulting mixture was partitioned between water and dichloromethane. The layers were separated and the organic layer was washed successively with 1 N hydrochloric acid, saturated aqueous sodium bicarbonate, and saturated aqueous sodium chloride. The organic layer was dried over magnesium sulfate, filtered, and concentrated under reduced pressure. The residue was either used directly for further reactions, or purified by chromatography or by crystallization from an appropriate solvent system before use.

The following compounds were prepared according to this sequence of procedures

4.1.5.3. *tert*-Butyl [3(*S*)-(4(*S*)-phenyloxazolidin-2-on-3-yl)-4(*R*)-(2-styryl)azetidin-2-on-1-yl]acetate (55). The imine prepared from 4.53 g (34.5 mmol) of glycine *tert*-butyl ester and *t*-cinnamaldehyde was combined with 2-(4(*S*)-phenyloxazolidin-2-on-3-yl) acetyl chloride (**4**) to give 5.5 g (30%) of **55** as colorless crystals (recrystallized, *n*-chlorobutane); mp 194–195 °C. ^{1}H NMR ($CDCl_3$) δ 1.39 (s, 9H); 3.43 (d, J = 18.0 Hz, 1H); 4.15 (dd, J = 7.5 Hz, J = 8.7 Hz, 1H); 4.24 (d, J = 18.0 Hz, 1H); 4.55–4.63 (m, 3H); 4.80 (dd, J = 7.7 Hz, J = 8.5 Hz, 1H); 6.05–6.13 (m, 1H); 6.64 (d, J = 16.0 Hz, 1H); 7.28–7.42 (m, 10H).

4.1.5.4. 2(*S*)-(*tert*-Butoxycarbonylmethyl)-2-[3(*S*)-(4(*S*)-phenyloxazolidin-2-on-3-yl)-4(*R*)-(2-styryl)azetidin-2-on-1-yl]acetic acid *N*-(3-trifluoromethylbenzyl)amide (56). Imine **36a** prepared from 1.52 g (4.39 mmol) of L-aspartic acid β-*tert*-butyl ester α-(3-trifluoromethyl)benzylamide (**35a**) and *t*-cinnamaldehyde was combined with 2-(4(*S*)-phenyloxazolidin-2-on-3-yl) acetyl chloride (**4**) to give 2.94 g of an orange-brown oil that gave, after flash column chromatography purification (70:30 hexanes/ethyl acetate), 2.06 g (70%) of **56** as a white solid; ^{1}H NMR ($CDCl_3$) δ 1.39 (s, 9H); 2.46 (dd, J = 11.1 Hz, J = 16.3 Hz, 1H); 4.18 (dd, J = 3.8 Hz, J = 16.4 Hz, 1H); 4.12–4.17 (m, 1H); 4.26 (d, J = 5.0 Hz, 1H); 4.45 (dd, J = 6.0 Hz, J = 14.9 Hz, 1H); 4.54 (dd, J = 5.3 Hz, J = 9.8 Hz, 1H); 4.58–4.66 (m, 3H); 4.69–4.75 (m, 1H); 4.81 (dd, J = 3.8 Hz, J = 11.1 Hz, 1H); 6.25 (dd, J = 9.6 Hz, J = 15.8 Hz, 1H); 6.70 (d, J = 15.8 Hz, 1H); 7.14–7.17 (m, 2H); 7.28–7.46 (m, 11H); 7.62 (s, 1H); 8.27–8.32 (m, 1H).

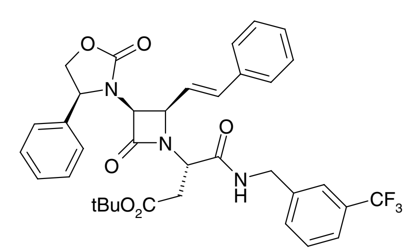

4.1.5.5. 2(*S*)-(*tert*-Butoxycarbonylmethyl)-2-[3(*S*)-(4(*S*)-phenyloxazolidin-2-on-3-yl)-4(*R*)-(2-styryl)azetidin-2-on-1-yl]acetic acid *N*-[4-(2-phenylethyl)]piperazinamide (57). Imine **36b** prepared from 4.20 g (11.6 mmol) of L-aspartic acid β-*tert*-butyl ester α-[4-(2-phenylethyl)]-piperazinamide (**35b**) and *t*-cinnamaldehyde was combined with 2-(4(*S*)-phenyloxazolidin-2-on-3-yl) acetyl chloride (**4**) to give 4.37 g (55%) of **57** as a white solid after flash column chromatography purification (50:50 hexanes/ethyl acetate); ^{1}H NMR ($CDCl_3$) δ 1.34 (s, 9H); 2.26–2.32 (m, 1H); 2.46–2.63 (m, 4H);

2.75–2.89 (m, 4H); 3.24–3.32 (m, 1H); 3.49–3.76 (m, 3H); 4.07–4.13 (m, 1H); 4.30 (d, $J = 4.6$ Hz, 1H); 4.22–4.48 (m, 1H); 4.55–4.61 (m, 1H); 4.69–4.75 (m, 1H); 5.04–5.09 (m, 1H); 6.15 (dd, $J = 9.3$ Hz, $J = 15.9$ Hz, 1H); 6.63 (d, $J = 15.8$ Hz, 1H); 7.18–7.42 (m, 15H).

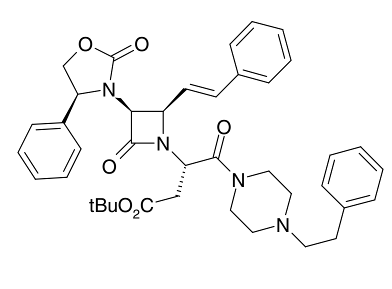

4.1.5.6. (*S*)-(*tert*-Butoxycarbonylethyl)-2-[3(*S*)-(4(*S*)-phenyloxazolidin-2-on-3-yl)-4(*R*)-(2-styryl)azetidin-2-on-1-yl]acetic acid *N*-(3-trifluoromethylbenzyl)amide (58). Imine **36c** prepared from 3.94 g (10.93 mmol) of L-glutamic acid γ-*tert*-butyl ester α-(3-trifluoromethyl)benzylamide (**35c**) and *t*-cinnamaldehyde was combined with 2-(4(*S*)-phenyloxazolidin-2-on-3-yl) acetyl chloride (**4**) to give 5.53 g (75%) of **58** as a white solid after flash column chromatography purification (70:30 hexanes/ethyl acetate); ^{1}H NMR ($CDCl_3$) δ 1.36 (s, 9H); 1.85–1.96 (m, 1H); 2.18–2.49 (m, 3H); 4.14–4.19 (m, 1H); 4.30 (d, $J = 4.9$ Hz, 2H); 4.44 (dd, $J = 6.1$ Hz, $J = 14.9$ Hz, 1H); 4.56–4.67 (m, 4H); 4.71–4.75 (m, 1H); 6.26 (dd, $J = 9.6$ Hz, $J = 15.8$ Hz, 1H); 6.71 (d, $J = 15.8$ Hz, 1H); 7.16–7.18 (m, 2H); 7.27–7.49 (m, 11H); 7.60 (s, 1H); 8.08–8.12 (m, 1H).

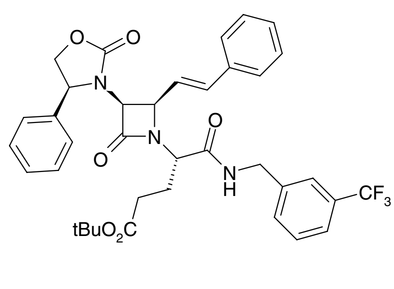

4.1.5.7. 2(*R*)-(*tert*-Butoxycarbonylmethyl)-2-[3(*S*)-(4(*S*)-phenyloxazolidin-2-on-3-yl)-4(*R*)-(2-styryl)azetidin-2-on-1-yl]acetic acid *N*-(3-trifluoromethylbenzyl)amide (59). Imine **40a** prepared from 0.973 g (2.81 mmol) of D-aspartic acid β-*tert*-butyl ester α-(3-trifluoromethyl)benzylamide (**39a**) and *t*-cinnamaldehyde was combined with 2-(4(*S*)-phenyloxazolidin-2-on-3-yl) acetyl chloride (**4**) to give 1.53 g (82%) of **59** as a white solid after flash column chromatography purification (70:30 hexanes/ethyl acetate); ^{1}H NMR ($CDCl_3$) δ 1.37 (s, 9H); 3.10 (dd, $J = 3.7$ Hz, $J = 17.8$ Hz, 1H); 3.20 (dd, $J = 10.7$ Hz, $J = 17.8$ Hz, 1H); 4.02 (dd, $J = 3.6$ Hz, $J = 10.6$ Hz, 1H); 4.11–4.17 (m, 1H); 4.24 (d, $J = 4.9$ Hz, 1H); 4.46 (dd, $J = 5.8$ Hz, $J = 15.1$ Hz, 1H); 4.58–4.67 (m, 3H); 4.70–4.76 (m, 1H); 6.27 (dd, $J = 9.5$ Hz, $J = 15.8$ Hz, 1H); 6.79 (d, $J = 15.8$ Hz, 1H); 7.25–7.50 (m, 13H); 7.63 (s, 1H); 8.50–8.54 (m, 1H).

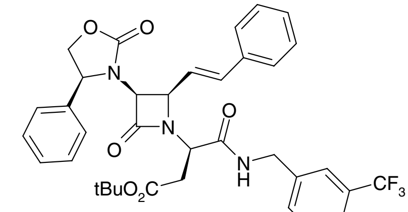

4.1.5.8. 2(*R*)-(*tert*-Butoxycarbonylmethyl)-2-[3(*S*)-(4(*S*)-phenyloxazolidin-2-on-3-yl)-4(*R*)-(2-styryl)azetidin-2-on-1-yl]acetic acid *N*-(2-fluoro-3-trifluoromethylbenzyl)amide (60). Imine **40b** prepared from 0.256 g (0.70 mmol) of D-aspartic acid β-*tert*-butyl ester α-(2-fluoro-3-trifluoromethyl)benzylamide (**39b**) and *t*-cinnamaldehyde was combined with 2-(4(*S*)-phenyloxazolidin-2-on-3-yl) acetyl (**4**) to give 0.287 g (60%) of **60** as a white solid after flash column chromatography purification (70:30 hexanes/ethyl acetate); ^{1}H NMR ($CDCl_3$) δ 1.38 (s, 9H); 3.12 (dd, $J = 4.0$ Hz, $J = 17.8$ Hz, 1H); 3.20 (dd, $J = 10.4$ Hz, $J = 17.8$ Hz, 1H); 4.05 (dd, $J = 3.9$ Hz, $J = 10.4$ Hz, 1H); 4.14 (dd, $J = J' = 8.2$ Hz, 1H); 4.25 (d, $J = 4.9$ Hz, 1H); 4.59–4.67 (m, 4H); 4.74 (t, $J = 8.3$ Hz, 1H); 6.36 (dd, $J = 9.6$ Hz, $J = 15.8$ Hz, 1H); 6.83 (d, $J = 15.8$ Hz, 1H); 7.02–7.07 (m, 1H); 7.28–7.55 (m, 12H); 8.44–8.48 (m, 1H).

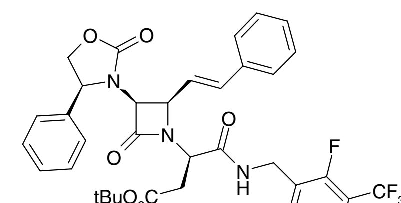

4.1.5.9. 2(*R*)-(*tert*-Butoxycarbonylmethyl)-2-[3(*S*)-(4(*S*)-phenyloxazolidin-2-on-3-yl)-4(*R*)-(2-styryl)azetidin-2-on-1-yl]acetic acid *N*-[(*S*)-α-methylbenzyl]amide (61). Imine **40c** prepared from 0.167 g (0.57 mmol) of D-aspartic acid β-*tert*-butyl ester [(*S*)-α-methylbenzyl]amide (**39c**) and *t*-cinnamaldehyde was combined with 2-(4(*S*)-phenyloxazolidin-2-on-3-yl) acetyl chloride (**4**) to give 0.219 g (63%) of **61** as a white solid after flash column chromatography purification (70:30 hexanes/ethyl acetate); ^{1}H NMR ($CDCl_3$) δ 1.35 (s, 9H); 1.56 (d, $J = 7.0$ Hz, 3H); 2.97 (dd, $J = 3.5$ Hz, $J = 18.0$ Hz, 1H); 3.15 (dd, $J = 11.0$ Hz, $J = 17.5$ Hz, 1H); 4.01 (dd, $J = 3.0$ Hz, $J = 11.0$ Hz, 1H); 4.14 (t, $J = 8.5$ Hz, 1H); 4.24 (d, $J = 5.0$ Hz, 1H); 4.57 (dd, $J = 5.0$ Hz, $J = 9.5$ Hz, 1H); 4.64 (t, $J = 8.8$ Hz, 1H); 5.07 (t, $J = 8.5$ Hz, 1H); 5.03–5.09 (m, 1H); 6.43 (dd, $J = 9.5$ Hz, $J = 16.0$ Hz, 1H); 6.83 (d, $J = 16.0$ Hz, 1H); 7.16–7.20 (m, 1H); 7.27–7.49 (m, 14H); 8.07–8.10 (m, 1H).

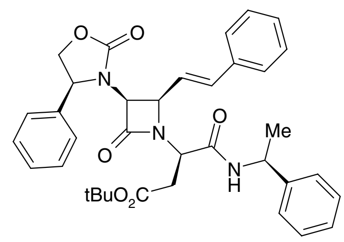

4.1.5.10. 2(*R*)-(*tert*-Butoxycarbonylmethyl)-2-[3(*S*)-(4(*S*)-phenyloxazolidin-2-on-3-yl)-4(*R*)-(2-styryl)azetidin-2-on-1-yl]acetic acid *N*-[(*R*)-α-methylbenzyl]amide (62). Imine **40d** prepared from 0.187 g (0.46 mmol) of D-aspartic acid β-*tert*-butyl ester [(*R*)-α-methylbenzyl]amide (**39d**) and *t*-cinnamaldehyde was combined with 2-(4(*S*)-phenyloxazolidin-2-on-3-yl) acetyl chloride (**4**) to give 0.25 g (64%) of **62** as a white solid after flash column chromatography purification (70:30 hexanes/ethyl acetate); ^{1}H NMR ($CDCl_3$) δ 1.36 (s, 9H); 1.59 (d, J = 7.1 Hz, 3H); 3.10 (dd, J = 3.5 Hz, J = 17.8 Hz, 1H); 3.22 (dd, J = 10.9 Hz, J = 17.8 Hz, 1H); 3.93 (dd, J = 3.5 Hz, J = 10.8 Hz, 1H); 4.14 (t, J = 8.1 Hz, 1H); 4.24 (d, J = 5.0 Hz, 1H); 4.58 (dd, J = 5.0 Hz, J = 9.5 Hz, 1H); 4.65 (t, J = 8.7 Hz, 1H); 4.74 (t, J = 8.2 Hz, 1H); 5.06–5.14 (m, 1H); 6.32 (dd, J = 9.5 Hz, J = 15.8 Hz, 1H); 6.74 (d, J = 15.8 Hz, 1H); 7.19–7.43 (m, 15H); 8.15–8.18 (m, 1H). ^{13}C NMR ($CDCl_3$) δ 21.84, 27.98, 35.44, 49.56, 54.81, 61.00, 61.98, 63.60, 71.00, 81.15, 121.25, 126.33, 126.80, 126.87, 127.18, 128.41, 128.75, 128.78, 129.69, 135.27, 135.91, 139.03, 143.99, 157.97, 162.99, 167.26, 170.94.

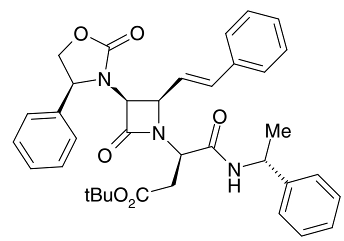

4.1.5.11. 2(*R*)-(*tert*-Butoxycarbonylmethyl)-2-[3(*S*)-(4(*S*)-phenyloxazolidin-2-on-3-yl)-4(*R*)-(2-styryl)azetidin-2-on-1-yl]acetic acid *N*-methyl-*N*-(3-trifluoromethylbenzyl)amide (63). Imine **40e** prepared from 0.195 g (0.41 mmol) of D-aspartic acid β-*tert*-butyl ester α-[*N*-methyl-*N*-(3-trifluoromethylbenzyl)]amide (**39e**) and *t*-cinnamaldehyde was combined with 2-(4(*S*)-phenyloxazolidin-2-on-3-yl) acetyl chloride (**4**) to give 0.253 g (69%) of **63** as a white solid after flash column chromatography purification (70:30 hexanes/ethyl acetate); ^{1}H NMR ($CDCl_3$) δ 1.36 (s, 9H); 2.53 (dd, J = 4.0 Hz, J = 17.0 Hz, 1H); 3.06 (dd, J = 10.8 Hz, J = 16.8 Hz, 1H); 3.13 (s, 3H); 4.12 (dd, J = 8.0 Hz, J = 9.0 Hz, 1H); 4.26 (d, J = 5.0 Hz, 1H); 4.38 (d, J = 15.0 Hz, 1H); 4.46 (dd, J = 5.0 Hz, J = 9.5 Hz, 1H); 4.56 (t, J = 6.8 Hz, 1H); 4.70–4.79 (m, 2H); 5.27 (dd, J = 4.0 Hz, J = 11.0 Hz, 1H); 6.22 (dd, J = 9.3 Hz, J = 15.8 Hz, 1H); 6.73 (d, J = 15.8 Hz, 1H); 7.33–7.45 (m, 14H).

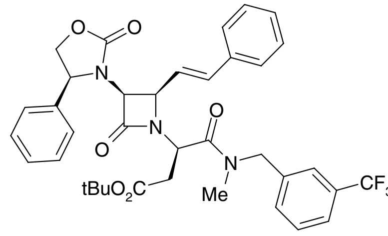

4.1.5.12. 2(*R*)-(*tert*-Butoxycarbonylmethyl)-2-[3(*S*)-(4(*S*)-phenyloxazolidin-2-on-3-yl)-4(*R*)-(2-styryl)azetidin-2-on-1-yl]acetic acid *N*-[(*S*)-1-(3-trifluoromethylphenyl)ethyl]amide (64). Imine **40f** prepared from 0.08 g (0.22 mmol) of D-aspartic acid β-*tert*-butyl ester [(*S*)-α-methylbenzyl]amide (**39f**) and *t*-cinnamaldehyde was combined with 2-(4(*S*)-phenyloxazolidin-2-on-3-yl) acetyl chloride (**4**) to give 53 mg (35%) of **64** as a white solid after flash column chromatography purification (70:30 hexanes/ethyl acetate); ^{1}H NMR ($CDCl_3$) δ 1.36 (s, 9H); 1.59 (d, J = 7.0 Hz, 3H); 3.00 (dd, J = 3.4 Hz, J = 17.8 Hz, 1H); 3.19 (dd, J = 11.0 Hz, J = 17.8 Hz, 1H); 4.01 (dd, J = 3.4 Hz, J = 11.0 Hz, 1H); 4.07–4.19 (m, 2H); 4.25 (d, J = 5.0 Hz, 1H); 4.58–4.78 (m, 3H); 5.09–5.16 (m, 1H); 6.44 (dd, J = 9.5 Hz, J = 15.8 Hz, 1H); 6.83 (d, J = 15.8 Hz, 1H); 7.19–7.47 (m, 13H); 7.63 (s, 1H), 8.26–8.29 (m, 1H).

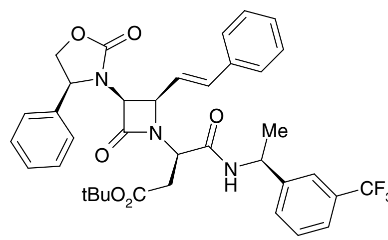

4.1.5.13. 2(*R*)-(*tert*-Butoxycarbonylmethyl)-2-[3(*S*)-(4(*S*)-phenyloxazolidin-2-on-3-yl)-4(*R*)-(2-styryl)azetidin-2-on-1-yl]acetic acid *N*-[(*R*)-1-(3-trifluoromethylphenyl)ethyl]amide (65). Imine **40g** prepared from 0.16 g (0.44 mmol) of D-aspartic acid β-*tert*-butyl ester [(*R*)-α-methylbenzyl]amide (**39g**) and *t*-cinnamaldehyde was combined with 2-(4(*S*)-phenyloxazolidin-2-on-3-yl) acetyl chloride (**4**) to give 0.166 g (55%) of **65** as a white solid after flash column chromatography purification (70:30 hexanes/ethyl acetate); ^{1}H NMR ($CDCl_3$) δ 1.36 (s, 9H); 1.60 (d, J = 7.1 Hz, 3H); 3.10 (dd, J = 3.7 Hz, J = 17.8 Hz, 1H); 3.19 (dd, J = 10.6 Hz, J = 17.8 Hz, 1H); 3.93 (dd, J = 3.7 Hz, J = 10.6 Hz, 1H); 4.16 (t, J = 8.1 Hz, 1H); 4.25 (d, J = 5.0 Hz, 1H); 4.58 (dd, J = 5.0 Hz, J = 9.5 Hz, 1H); 4.67 (t, $J = 8.6$ Hz, 1H); 4.74 (t, $J = 8.2$ Hz, 1H); 5.10–5.19 (m, 1H); 6.27 (dd, $J = 9.5$ Hz, $J = 15.8$ Hz, 1H); 6.74 (d, $J = 15.8$ Hz, 1H); 7.17–7.59 (m, 13H); 7.75 (s, 1H), 8.25–8.27 (m, 1H).

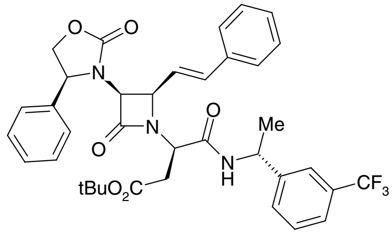

4.1.5.14. 2(*R*)-(*tert*-Butoxycarbonylethyl)-2-[3(*S*)-(4(*S*)-phenyloxazolidin-2-on-3-yl)-4(*R*)-(2-styryl)azetidin-2-on-1-yl]acetic acid *N*-(3-trifluoromethylbenzyl)amide (66). Imine **40h** prepared from 1.15 g (3.20 mmol) of D-glutamic acid γ-*tert*-butyl ester α-(3-trifluoromethyl)benzylamide (**39h**) and *t*-cinnamaldehyde was combined with 2-(4(*S*)-phenyloxazolidin-2-on-3-yl) acetyl chloride (**4**) to give 1.84 g (85%) of **66** as a white solid after flash column chromatography purification (70:30 hexanes/ethyl acetate); ^{1}H NMR ($CDCl_3$) δ 1.37 (s, 9H); 2.23–2.39 (m, 4H); 3.71–3.75 (m, 1H); 4.13–4.18 (m, 1H); 4.31 (d, $J = 4.9$ Hz, 1H); 4.44–4.51 (m, 2H); 4.56–4.68 (m, 2H); 4.71–4.76 (m, 1H); 6.26 (dd, $J = 9.5$ Hz, $J = 15.8$ Hz, 1H); 6.71 (d, $J = 15.8$ Hz, 1H); 7.25–7.52 (m, 13H); 7.63 (s, 1H); 8.25–8.30 (m, 1H).

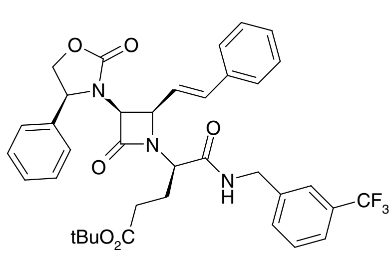

4.1.5.15. *tert*-Butyl 2(*S*)-(2-(4-cyclohexylpiperazin-1-ylcarbonyl)ethyl)-2-[3(*S*)-(4(*S*)-phenyloxazolidin-2-on-3-yl)-4(*R*)-(2-styryl)azetidin-2-on-1-yl]acetate (67). Imine **45a** prepared from 1.282 g (3.63 mmol) of L-glutamic acid α-*tert*-butyl ester γ-(4-cyclohexyl)piperazinamide (**44a**) and *t*-cinnamaldehyde was combined with 2-(4(*S*)-phenyloxazolidin-2-on-3-yl) acetyl chloride (**4**) to give 1.946 g (80%) of **67** as a white solid after flash column chromatography purification (50:50 hexanes/ethyl acetate); ^{1}H NMR ($CDCl_3$) δ 1.15–1.26 (m, 6H); 1.39 (s, 9H); 1.55–1.64 (m, 2H); 1.77–1.83 (m, 3H); 2.22–2.35 (m, 2H); 2.40–2.50 (m, 6H); 2.75–2.79 (m, 1H); 3.43–3.48 (m, 1H); 3.56–3.60 (m, 2H); 3.75–3.79 (m, 1H); 4.10 (t, $J = 8.3$ Hz, 1H); 4.31–4.35 (m, 2H); 4.58 (t, $J = 8.8$ Hz, 1H); 4.73 (t, $J = 8.4$ Hz, 1H); 6.17 (dd, $J = 8.6$ Hz, $J = 16.0$ Hz, 1H); 6.65 (d, $J = 16.0$ Hz, 1H); 7.27–7.42 (m, 10H).

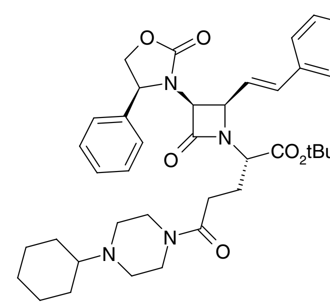

4.1.6. General procedure for acylation of an (azetidin-2-on-1-yl)acetate. A solution of (azetidin-2-on-1-yl)acetate in tetrahydrofuran (0.22 M in azetidinone) is cooled to −78 °C and treated with lithium bis(trimethylsilyl)amide (2.2 equiv). The resulting anion is treated with an appropriate acyl halide (1.1 equiv). Upon complete conversion of the azetidinone, the reaction is quenched with saturated aqueous ammonium chloride and partitioned between ethyl acetate and water. The organic phase is washed sequentially with 1 N hydrochloric acid, saturated aqueous sodium bicarbonate, and saturated aqueous sodium chloride. The resulting organic layer is dried (magnesium sulfate) and evaporated. The residue is purified by silica gel chromatography with an appropriate eluent, such as 60:40 hexanes/ethyl acetate.

The following compound was prepared according to this procedure:

4.1.6.1. 2,2,2-Trichloroethyl 2(*R*,*S*)-(*tert*-butoxycarbonyl)-2-[3(*S*)-(4(*S*)-phenyloxazolidin-2-on-3-yl)-4(*R*)-(2-styryl)azetidin-2-on-1-yl]acetate (30). Azetidinone **55**, 9.0 g (20 mmol), was acylated with 4.2 g (20 mmol) of trichloroethylchloroformate to give 7.0 g (56%) of **30** as a white solid; mp 176–178 °C. ^{1}H NMR ($CDCl_3$) δ 1.31–1.34 and 1.43–1.46 (m and m′, 9H); 4.12–4.18 (m, 1H); 4.53–4.90 (m; 6H); 5.18–5.24 (m, 1H); 6.10–6.18 (m, 1H); 6.61–6.66 (m, 1H); 7.28–7.41 (m, 10H).

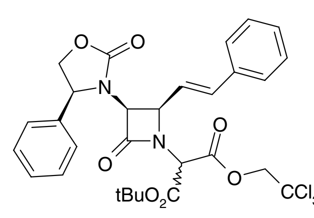

4.1.6.2. 2(RS)-(*tert*-Butoxycarbonyl)-2-[3(*S*)-(4(*S*)-phenyloxazolidin-2-on-3-yl)-4(*R*)-(2-styryl)azetidin-2-on-1-yl]acetic acid *N*-(3-trifluoromethylbenzyl)amide (31). A solution of 0.20 g (0.32 mmol) of **30** and 52 μL (0.36 mmol) of (3-trifluoromethylbenzyl)amine in THF was heated at reflux. Upon complete conversion (TLC), the solvent was evaporated and the residue was crystallized (chloroform/hexane) to give 0.17 g (82%)

of **31** as a white solid; mp 182–184 °C. ^{1}H NMR ($CDCl_3$) δ 1.36–1.44 (m, 9H); 4.13–4.14–4.91 (m; 8H); 6.23–6.31 (m, 1H); 6.65–6.78 (m, 1H); 7.20–7.60 (m, 14H); 7.88–7.92 and 8.08–8.12 (m and m′, 1H). Anal. Calcd for $C_{35}H_{34}F_3N_3O_6$: C, 64.71; H, 5.28; N, 6.47. Found: C, 64.78; H, 5.31; N, 6.36.

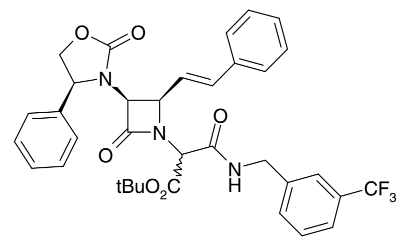

4.1.7. General procedure for hydrolysis of a *tert*-butyl ester. A solution of *tert*-butyl ester derivative in formic acid, typically 1 g in 10 mL, is stirred at ambient temperature until no more ester is detected by thin-layer chromatography (dichloromethane 95%/methanol 5%), a typical reaction time being around 3 h. The formic acid is then evaporated under reduced pressure to yield the corresponding carboxylic acid.

The following compounds were prepared according to this procedure

4.1.7.1. 2(R,S)-(Carboxy)-2-[3(*S*)-(4(*S*)-phenyloxazolidin-2-on-3-yl)-4(*R*)-(2-styryl)azetidin-2-on-1-yl]acetic acid *N*-(3-trifluoromethylbenzyl)amide (32). Compound **31** (0.30 g, 0.46 mmol) was hydrolyzed to give 0.27 g (quantitative yield) of **32** as an off-white solid; ^{1}H NMR ($CDCl_3$) δ 4.17–5.28 (m, 9H); 6.21–6.29 (m, 1H), 6.68–6.82 (m, 1H); 7.05–7.75 (m, 13H); 9.12–9.18 (m, 1H).

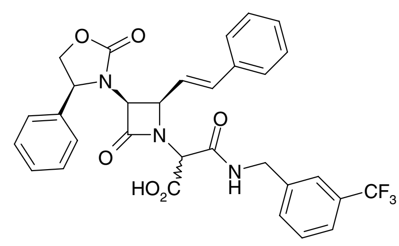

4.1.7.2. 2(*S*)-(Carboxymethyl)-2-[3(*S*)-(4(*S*)-phenyloxazolidin-2-on- 3-yl)-4(*R*)-(2-styryl)azetidin-2-on-1-yl]acetic acid *N*-(3-trifluoromethylbenzyl)amide (68). Compound **56** (1.72 g, 2.59 mmol) was hydrolyzed to give 1.57 g (quantitative yield) of **68** as an off-white solid; ^{1}H NMR ($CDCl_3$) δ 2.61 (dd, J = 9.3 Hz, J = 16.6 Hz, 1H); 3.09–3.14 (m, 1H); 4.10–4.13 (m, 1H); 4.30 (d, J = 4.5 Hz, 1H); 4.39–4.85 (m, 6H); 6.20 (dd, J = 9.6 Hz, J = 15.7 Hz, 1H); 6.69 (d, J = 15.8 Hz, 1H); 7.12–7.15 (m, 2H); 7.26–7.50 (m, 11H); 7.61 (s, 1H); 8.41–8.45 (m, 1H).

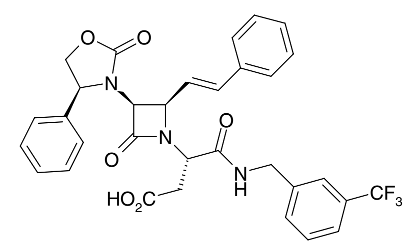

4.1.7.3. 2(*S*)-(Carboxymethyl)-2-[3(*S*)-(4(*S*)-phenyloxazolidin-2-on-3-yl)-4(*R*)-(2-styryl)azetidin-2-on-1-yl]acetic acid *N*-[4-(2-phenylethyl)]piperazinamide (69). Compound **57** (1.88 g, 2.78 mmol) was hydrolyzed to give 1.02 g (60%) of **69** as an off-white solid; ^{1}H NMR ($CDCl_3$) δ 2.63 (dd, J = 6.0 Hz, J = 16.5 Hz, 1H); 2.75–2.85 (m, 1H); 3.00 (dd, J = 8.2 Hz, J = 16.6 Hz, 1H); 3.13–3.26 (m, 4H); 3.37–3.56 (m, 4H); 3.86–4.00 (m, 1H); 4.05–4.11 (m, 1H); 4.24 (d, J = 5.0 Hz, 1H); 4.46–4.66 (m, 1H); 4.65–4.70 (m, 1H); 5.10–5.15 (m, 1H); 6.14 (dd, J = 9.3 Hz, J = 15.9 Hz, 1H); 6.71 (d, J = 15.9 Hz, 1H); 7.22–7.41 (m, 15H); 12.02 (s, 1H).

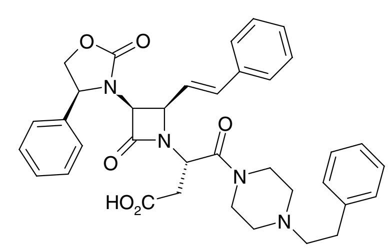

4.1.7.4. 2(*S*)-(Carboxyethyl)-2-[3(*S*)-(4(*S*)-phenyloxazolidin-2-on-3-yl)-4(*R*)-(2-styryl)azetidin-2-on-1-yl]acetic acid *N*-(3-trifluoromethylbenzyl)amide (70). Compound **58** (4.97 g, 7.34 mmol) was hydrolyzed to give 4.43 g (97%) of **70** as an off-white solid; ^{1}H NMR ($CDCl_3$) δ 1.92–2.03 (m, 1H); 2.37–2.51 (m, 3H); 4.13–4.19 (m, 1H); 3.32 (d, J = 4.9 Hz, 1H); 4.35–4.39 (m, 1H); 4.44 (dd, J = 5.9 Hz, J = 14.9 Hz, 1H); 4.50–4.57 (m, 2H); 4.61–4.67 (m, 1H); 4.70–4.76 (m, 1H); 6.24 (dd, J = 9.6 Hz, J = 15.8 Hz, 1H); 6.70 (d, J = 15.8 Hz, 1H); 7.18–7.47 (m, 14H).

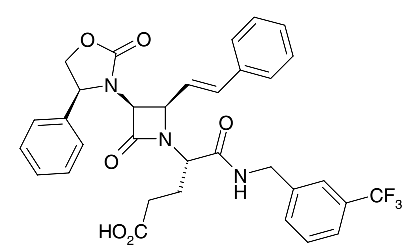

4.1.7.5. 2(*R*)-(Carboxymethyl)-2-[3(*S*)-(4(*S*)-phenyloxazolidin-2-on-3-yl)-4(*R*)-(2-styryl)azetidin-2-on-1-yl]acetic acid *N*-(3-trifluoromethylbenzyl)amide (71). Compound

59 (1.51 g, 2.27 mmol) was hydrolyzed to give 1.38 g (quantitative yield) of **71** as an off-white solid; ^{1}H NMR (CD_3OD) δ 2.93 (dd, J = 5.5 Hz, J = 17.0 Hz, 1H); 2.99 (dd, J = 9.0 Hz, J = 17.0 Hz, 1H); 4.17 (dd, J = 7.0 Hz, J = 9.0 Hz, 1H); 4.36 (dd, J = 5.5 Hz, J = 9.0 Hz, 1H); 4.40–4.45 (m, 2H) 4.55 (d, J = 15.5 Hz, 1H); 4.65 (dd, J = 5.0 Hz, J = 9.0 Hz, 1H); 4.70 (dd, $J = J'$ = 9.0 Hz, 1H); 4.89 (dd, J = 7.0 Hz, J = 9.0 Hz, 1H); 6.26 (dd, J = 9.0 Hz, J = 16.0 Hz, 1H); 6.83 (d, J = 16.0 Hz, 1H); 7.24–7.32 (m, 5H); 7.38–7.48 (m, 6H); 7.51–7.57 (m, 2H); 7.64 (s, 1H). ^{13}C NMR (CD_3OD) δ 43.82, 55.92, 62.01, 63.34, 64.52, 72.58, 123.03, 124.97 (q, $^3J_{C-F}$, 3.8Hz, 1C), 125.54 (q, $^3J_{C-F}$, 3.8 Hz, 1C), 127.82, 128.55, 129.66, 129.81, 130.34, 130.44, 130.54, 131.77 (q, $^1J_{C-F}$, 32.3 Hz, CF_3), 132.3–132.4 (m, 1C), 137.23, 138.42, 139.71, 141.19, 160.28, 166.12, 171.23.

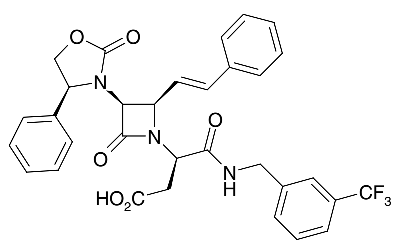

4.1.7.6. 2(*R*)-(Carboxymethyl)-2-[3(*S*)-(4(*S*)-phenyloxazolidin-2-on-3-yl)-4(*R*)-(2-styryl)azetidin-2-on-1-yl]acetic acid *N*-(2-fluoro-3-trifluoromethylbenzyl)carboxamide (72). Compound **60** (0.26 g, 0.38 mmol) was hydrolyzed to give 0.238 g (quantitative yield) of **72** as an off-white solid; ^{1}H NMR ($CDCl_3$) δ 3.27 (d, J = 7.2 Hz, 1H); 4.06 (t, J = 7.2 Hz, 1H); 4.15 (t, J = 8.1 Hz, 1H); 4.27 (d, J = 4.8 Hz, 1H); 4.56–4.76 (m, 5H); 6.34 (dd, J = 9.5 Hz, J = 15.7 Hz, 1H); 6.80 (d, J = 15.7 Hz, 1H); 7.06 (t, J = 7.7 Hz, 1H); 7.31–7.54 (m, 12H); 8.58 (t, J = 5.9 Hz, 1H).

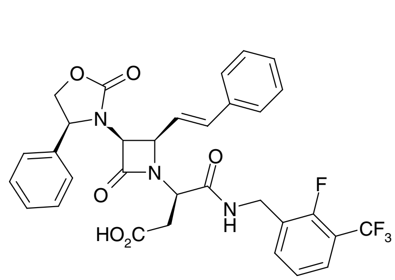

4.1.7.7. 2(*R*)-(Carboxymethyl)-2-[3(*S*)-(4(*S*)-phenyloxazolidin-2-on-3-yl)-4(*R*)-(2-styryl)azetidin-2-on-1-yl]acetic acid *N*-[(*S*)-α-methylbenzyl]amide (73). Compound **61** (0.215 g, 0.35 mmol) was hydrolyzed to give 0.195 g (quantitative yield) of **73** as an off-white solid; ^{1}H NMR ($CDCl_3$) δ 1.56 (d, J = 7.0 Hz, 1H); 3.10 (dd, J = 4.5 Hz, J = 17.9 Hz, 1H); 3.18 (dd, J = 9.8 Hz, J = 17.9 Hz, 1H); 4.00 (dd, J = 4.5 Hz, J = 9.7 Hz, 1H); 4.14 (t, J = 8.2 Hz, 1H); 4.26 (d, J = 4.7 Hz, 1H); 5.02–5.09 (m, 1H); 6.41 (dd, J = 9.4 Hz, J = 15.8 Hz, 1H); 6.78 (d, J = 15.8 Hz, 1H); 7.18 (t, J = 7.3 Hz, 1H); 7.26–7.43 (m, 14H); 8.29 (d, J = 8.2 Hz, 1H).

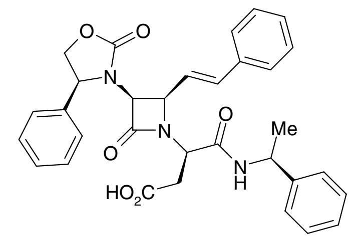

4.1.7.8. 2(*R*)-(Carboxymethyl)-2-[3(*S*)-(4(*S*)-phenyloxazolidin-2-on-3-yl)-4(*R*)-(2-styryl)azetidin-2-on-1-yl]acetic acid *N*-[(*R*)-α-methylbenzyl]amide (74). Compound **62** (0.22 g, 0.35 mmol) was hydrolyzed to give 0.20 g (quantitative yield) of **74** as an off-white solid; ^{1}H NMR ($CDCl_3$) δ 1.59 (d, J = 7.0 Hz, 1H); 3.25 (d, J = 7.0 Hz, 2H); 3.92 (t, J = 7.3 Hz, 1H); 4.15 (t, J = 8.3 Hz, 1H); 4.26 (d, J = 5.0 Hz, 1H); 4.52 (dd, J = 4.8 Hz, J = 9.3 Hz, 1H); 4.65 (t, J = 8.8 Hz, 1H); 4.72 (t, J = 8.3 Hz, 1H); 5.07–5.28 (m, 1H); 6.29 (dd, J = 9.5 Hz, J = 15.6 Hz, 1H); 6.71 (d, J = 16.0 Hz, 1H); 7.20–7.43 (m, 15H); 8.31 (d, J = 8.0 Hz, 1H). ^{13}C NMR ($CDCl_3$) δ 21.73, 34.23, 49.83, 54.37, 61.02, 62.04, 63.64, 71.10, 120.71, 126.36, 126.91, 126.96, 127.20, 128.49, 128.78, 128.89, 129.74, 135.16, 135.84, 139.43, 143.68, 158.06, 163.37, 167.38, 174.53.

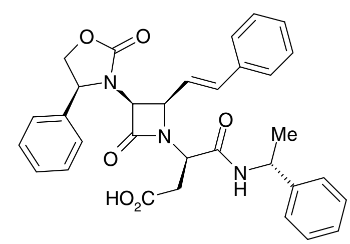

4.1.7.9. 2(*R*)-(Carboxymethyl)-2-[3(*S*)-(4(*S*)-phenyloxazolidin-2-on-3-yl)-4(*R*)-(2-styryl)azetidin-2-on-1-yl]acetic acid *N*-methyl-*N*-(3-trifluoromethylbenzyl)amide (75). Compound **63** (0.253 g, 0.37 mmol) was hydrolyzed to give 0.232 g (quantitative yield) of **75** as an off-white solid; ^{1}H NMR ($CDCl_3$) δ 3.07–3.15 (m, 4H); 4.13 (t, J = 8.2 Hz, 1H); 4.30 (d, J = 4.9 Hz, 1H); 4.46–4.78 (m, 5H); 5.23 (dd, J = 4.6 Hz, J = 9.7 Hz, 1H); 6.20 (dd, J = 9.4 Hz, J = 15.9 Hz, 1H); 6.73 (d, J = 15.9 Hz, 1H); 7.25–7.43 (m, 14H).

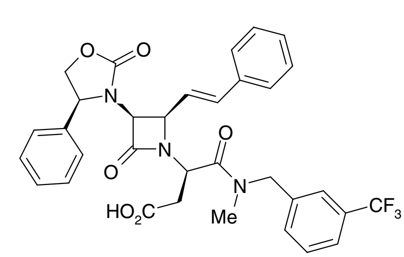

4.1.7.10. 2(*R*)-(Carboxylmethyl)-2-[3(*S*)-(4(*S*)-phenyloxazolidin-2-on-3-yl)-4(*R*)-(2-styryl)azetidin-2-on-1-yl]acetic acid *N*-[(*S*)-1-(3-trifluoromethylphenyl)ethyl]amide (76). Compound **64** (38.5 mg, 0.06 mmol) was hydrolyzed to give 35 mg (quantitative yield) of **76** as an off-white solid. ^{1}H NMR ($CDCl_3$) δ 1.58 (d, $J = 7.0$ Hz, 3H); 3.07–3.25 (m, 2H); 4.02 (dd, $J = 4.8$ Hz, $J = 9.5$ Hz, 1H); 4.15 (t, $J = 8.2$ Hz, 1H); 4.27 (d, $J = 4.8$ Hz, 1H); 4.57 (dd, $J = 4.8$ Hz, $J = 9.4$ Hz, 1H); 4.61–4.77 (m, 2H); 5.07–5.29 (m, 1H); 6.41 (dd, $J = 9.4$ Hz, $J = 15.8$ Hz, 1H); 6.79 (d, $J = 15.8$ Hz, 1H); 7.26–7.45 (m, 13H); 7.63 (s, 1H); 8.41 (d, $J = 8.1$ Hz, 1H).

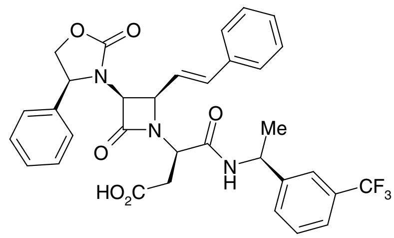

4.1.7.11. 2(*R*)-(Carboxylmethyl)-2-[3(*S*)-(4(*S*)-phenyloxazolidin-2-on- 3-yl)-4(*R*)-(2-styryl)azetidin-2-on-1-yl]acetic acid *N*-[(*R*)-1-(3-trifluoromethylphenyl)ethyl]amide (77). Compound **65** (166 mg, 0.24 mmol) was hydrolyzed to give 152 mg (quantitative yield) of **77** as an off-white solid. ^{1}H NMR ($CDCl_3$) δ 1.60 (d, $J = 7.0$ Hz, 3H); 3.08–3.26 (m, 2H); 3.93 (dd, $J = 4.7$ Hz, $J = 9.5$ Hz, 1H); 4.17 (t, $J = 8.1$ Hz, 1H); 4.26 (d, $J = 4.7$ Hz, 1H); 4.54 (dd, $J = 4.7$ Hz, $J = 9.4$ Hz, 1H); 4.62–4.76 (m, 2H); 5.06–5.28 (m, 1H); 6.24 (dd, $J = 9.4$ Hz, $J = 15.8$ Hz, 1H); 6.73 (d, $J = 15.8$ Hz, 1H); 7.28–7.58 (m, 13H); 7.74 (s, 1H); 8.40 (d, $J = 7.4$ Hz, 1H).

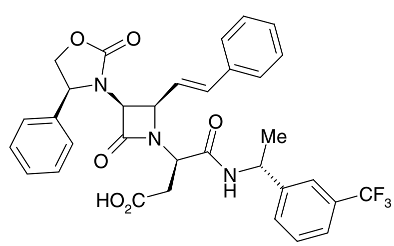

4.1.7.12. 2(*R*)-(Carboxyethyl)-2-[3(*S*)-(4(*S*)-phenyloxazolidin-2-on-3-yl)-4(*R*)-(2-styryl)azetidin-2-on-1-yl]acetic acid *N*-(3-trifluoromethylbenzyl)amide (78). Compound **66** (0.604 g, 0.89 mmol) was hydrolyzed to give 0.554 g (quantitative yield) of **78** as an off-white solid; ^{1}H NMR ($CDCl_3$) δ 2.27–2.34 (m, 4H); 4.10–4.30 (m, 2H); 4.30 (d, $J = 4.3$ Hz, 1H); 4.40–4.64 (m, 4H); 4.47 (t, $J = 8.1$ Hz, 1H); 6.22 (dd, $J = 9.4$ Hz, $J = 15.7$ Hz, 1H); 6.70 (d, $J = 15.7$ Hz, 1H); 7.25–7.57 (m, 14H); 8.32–8.36 (m, 1H).

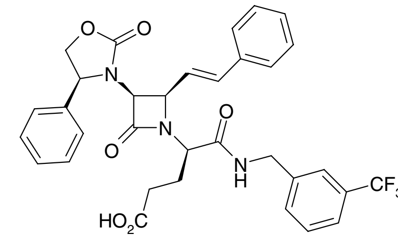

4.1.7.13. 2(*S*)-(2-(4-Cyclohexylpiperazin-1-ylcarbonyl)ethyl)-2-[3(*S*)-(4(*S*)- phenyloxazolidin-2-on-3-yl)-4(*R*)-(2-styryl)azetidin-2-on-1-yl]acetic acid (79). Compound **67** (0.787 g, 1.28 mmol) was hydrolyzed to give 0.665 g (92%) of **79** as an off-white solid; ^{1}H NMR ($CDCl_3$) δ 1.05–1.13 (m, 1H); 1.20–1.40 (m, 5H); 1.60–1.64 (m, 1H); 1.79–1.83 (m, 2H); 2.00–2.05 (m, 2H); 2.22–2.44 (m, 3H); 2.67–2.71 (m, 1H); 2.93–3.01 (m, 4H); 3.14–3.18 (m, 1H); 3.38–3.42 (m, 1H); 3.48–3.52 (m, 1H); 3.64–3.69 (m, 1H); 4.06–4.14 (m, 2H); 4.34–4.43 (m, 2H); 4.56 (t, $J = 8.8$ Hz, 1H); 4.73 (t, $J = 8.4$ Hz, 1H); 6.15 (dd, $J = 9.1$ Hz, $J = 16.0$ Hz, 1H); 6.65 (d, $J = 16.0$ Hz, 1H); 7.25–7.42 (m, 10H).

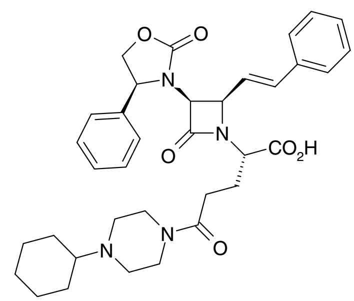

The compounds shown in Table 1, Figure 18 were prepared using the procedure shown in Section 4.1.3, except that *N*-benzyloxycarbonyl-D-aspartic acid β-*tert*-butyl ester monohydrate was replaced with **32**, and 3-(trifluoromethyl)benzylamine was replaced with the appropriate amine HNR_1R_2; all compounds exhibited an ^{1}H NMR spectrum consistent with the assigned structure.

4.1.8. Aspartic acid derivatives. The compounds shown in Table 2, Figure 19 were prepared using the procedure shown in Section 4.1.3, except that *N*-benzyloxycarbonyl-D-aspartic acid β-*tert*-butyl ester monohydrate was replaced with **68**, and 3-(trifluoromethyl)benzylamine was replaced with the appropriate amine HNR_1R_2; all compounds exhibited an ^{1}H NMR spectrum consistent with the assigned structure.

The compounds shown in Table 3, Figure 20 were prepared using the procedure shown in Section 4.1.3, except that *N*-benzyloxycarbonyl-D-aspartic acid β-*tert*-butyl ester monohydrate was replaced with **69**, and 3-(trifluoromethyl)benzylamine was replaced with the appropriate amine HNR_1R_2; all compounds exhibited an ^1H NMR spectrum consistent with the assigned structure.

The compounds shown in Table 4, Figure 21 were prepared using the procedure shown in Section 4.1.3, except that *N*-benzyloxycarbonyl-D-aspartic acid β-*tert*-butyl ester monohydrate was replaced with **71**, and 3-(trifluoromethyl)benzylamine was replaced with the appropriate amine HNR_1R_2; all compounds exhibited an ^1H NMR spectrum consistent with the assigned structure (Table 5, HRMS and Ki data).

4.1.9. A typical example being 41: 2(*R*)-[[4-(piperidin-1-yl)piperidin-1-yl]carbonylmethyl]-2-[3(*S*)-(4(*S*)-phenyloxazolidin-2-on-3-yl)-4(*R*)-(2-styryl)azetidin-2-on-1-yl]acetic acid *N*-(3-trifluoromethylbenzyl)amide. Compound **41** was obtained as an off-white solid after flash silica gel column chromatography (CH_2Cl_2 99% and down to 90%/MeOH 1% and up to 10%, NH_4OH < 1%). ^1H NMR ($CDCl_3$) δ 1.34–1.54 (m, 4H); 1.60–1.74 (m, 4H); 1.84–1.95 (m, 2H); 2.42–2.66 (m, 6H); 2.87–2.95 (m, 1H); 3.13–3.19 (m, 1H); 3.30–3.37 (m, 1H); 3.77–3.84 (m, 1H); 4.09–4.18 (m, 2H); 4.22 (dd, J = 4.5 Hz, 1H); 4.43–4.56 (m, 2H); 4.58–4.66 (m, 2H); 4.70–4.74 (m, 2H); 6.25–6.32 (m, 1H); 6.80–6.85 (m, 1H); 7.25–7.53 (m, 13H); 7.64 (s, 1H); 8.62–8.69 (m, 1H). ^{13}C NMR ($CDCl_3$) δ 24.02, 25.30, 27.10, 29.63, 33.72/33.75, 41.18/41.37, 43.15, 44.56/44.67, 49.90/49.98, 54.79/54.92, 61.16, 61.94/61.98, 62.50/62.62, 63.30/63.34, 71.06, 120.69, 123.05, 123.77 (q, $^3J_{C-F}$, 3.5 Hz, 1C), 124.52 (q, $^3J_{C-F}$, 3.8 Hz, 1C), 125.21, 126.78, 127.27, 128.77, 128.85, 128.92, 129.65, 129.74, 130.55, 130.76/130.79, 135.27, 135.68/135.72, 139.43, 139.48/139.53, 158.30, 163.18, 168.07/168.34, 169.41. HRMS (FAB) calcd for $C_{42}H_{47}F_3N_5O_5$ 758.3529, found 758.3510 $(M+H)^+$.

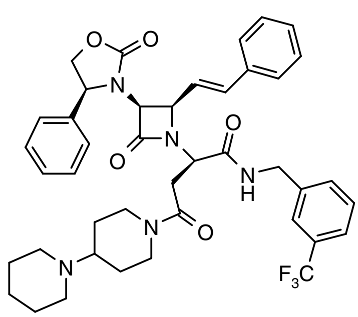

4.1.9.1. 2(*R*)-[[4-(Piperidin-1-yl)piperidin-1-yl]carbonylmethyl]-2-[3(*S*)-(4(*S*)-phenyloxazolidin-2-on-3-yl)-4(*R*)-(2-styryl)azetidin-2-on-1-yl]acetic acid *N*-(2-fluoro-3-trifluoromethylbenzyl)amide (102). Compound **102** was prepared using the procedure shown in Section 4.1.3, except that *N*-benzyloxycarbonyl-D-aspartic acid β-*tert*-butyl ester monohydrate was replaced with **72** and 3-(trifluoromethyl)benzylamine was replaced with 4-(1-piperidinyl)piperidine. Compound **102** exhibited a ^1H NMR spectrum consistent with the assigned structure. HRMS (FAB) calcd for $C_{42}H_{46}F_4N_5O_5$ 776.3435, found 776.3463 $(M+H)^+$.

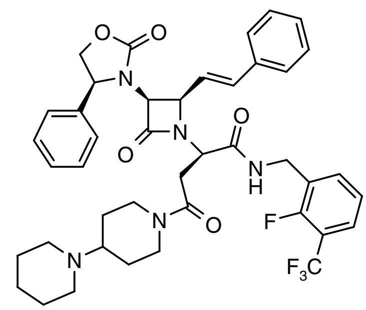

4.1.9.2. 2(*R*)-[[4-(Piperidin-1-yl)piperidin-1-yl]carbonylmethyl]-2-[3(*S*)-(4(*S*)-phenyloxazolidin-2-on-3-yl)-4(*R*)-(2-styryl)azetidin-2-on-1-yl]acetic acid *N*-[(*S*)-α-methylbenzyl]amide (52). Compound **52** was prepared using the procedure shown in Section 4.1.3, except that *N*-benzyloxycarbonyl-D-aspartic acid β-*tert*-butyl ester monohydrate was replaced with **73** and 3-(trifluoromethyl)benzylamine was replaced with 4-(1-piperidinyl)piperidine. Compound **52** exhibited a ^1H NMR spectrum consistent with the assigned structure. HRMS (FAB) calcd for $C_{42}H_{50}N_5O_5$ 704.3812, found 704.3806 $(M+H)^+$.

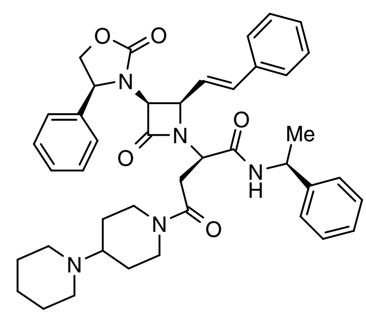

4.1.9.3. 2(*R*)-[[4-[2-(1-Piperidinyl)ethyl]piperidin-1-yl]carbonylmethyl]-2-[3(*S*)-(4(*S*)-phenyloxazolidin-2-on-3-yl)-4(*R*)-(2-styryl)azetidin-2-on-1-yl]acetic acid *N*-[(*S*)-α-methylbenzyl]amide (103). Compound **103** was prepared using the procedure shown in Section 4.1.3, except that *N*-benzyloxycarbonyl-D-aspartic acid β-*tert*-butyl ester monohydrate was replaced with **73** and 3-(trifluoromethyl)benzylamine was replaced with 4-[2-(1-piperidinyl)ethyl]piperidine. Compound **103** exhibited a ^1H NMR spectrum consistent with the assigned structure. HRMS (FAB) calcd for $C_{44}H_{54}N_5O_5$ 732.4125, 732.4108 $(M+H)^+$.

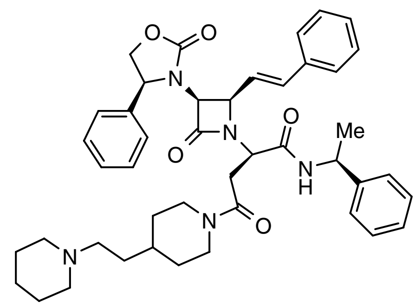

Table 1. Structures, HRMS (FAB), V1a K_i values

Compound	HNR_1R_2	Calcd for and equal to	Found: (M+H)	K_i (nM)
33	4-[2-(1-Piperidinyl)ethyl]piperidine	$C_{43}H_{49}F_3N_5O_5$ 772.3686	772.3711	1.17
80	4-(1-Piperidinyl)piperidine	$C_{41}H_{45}F_3N_5O_5$ 744.3373	744.3399	3.39
81	4-Butylpiperazine	$C_{39}H_{43}F_3N_5O_5$ 718.3216	718.3194	6.5
82	1-Benzyl-4-aminopiperidine	$C_{43}H_{43}F_3N_5O_5$ 766.3216	766.3191	13.3
83	4-Isopropylpiperazine	$C_{38}H_{41}F_3N_5O_5$ 704.3060	704.3038	18.2
84	4-Cyclohexylpiperazine	$C_{41}H_{45}F_3N_5O_5$ 744.3377	744.3367	26.4
85	2-(1-Piperidinyl)ethylamine	$C_{38}H_{41}F_3N_5O_5$ 704.3060	704.3064	61

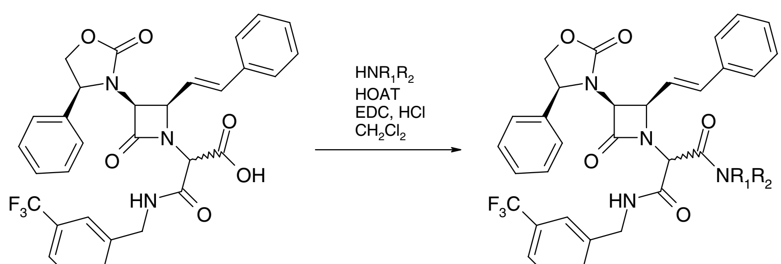

Figure 18. Aminomalonic acid derivatives.

Table 2. Structures, HRMS (FAB), V1a K_i values

Compound	HNR_1R_2	Calcd for and equal to	Found: (M+H)	K_i (nM)
37	1-Benzyl-4-aminopiperidine	$C_{44}H_{45}F_3N_5O_5$ 780.3373	780.3356	1.13
42	4-(1-Piperidinyl)piperidine	$C_{42}H_{47}F_3N_5O_5$ 758.3529	758.3554	1.89
86	(+)-3(*S*)-1-Benzyl-3-aminopyrrolidine	$C_{43}H_{43}F_3N_5O_5$ 766.3216	766.3201	3.60
87	4-Benzylhomopiperazine	$C_{45}H_{47}F_3N_5O_5$ 794.3524	794.3511	5.12
88	4-[2-(1-Piperidinyl)ethyl]piperidine	$C_{44}H_{51}F_3N_5O_5$ 786.3842	786.3860	6.00
89	1-Benzyl-4-aminopiperidine[a] (Zone B = 2-phenylethyl)	$C_{44}H_{47}F_3N_5O_5$ 782.3534	782.3535	23
90	4-(1-Pyrrolidinyl)piperazine	$C_{41}H_{45}F_3N_5O_5$ 744.3373	744.3355	~30
91	4-Cyclohexylpiperazine	$C_{42}H_{47}F_3N_5O_5$ 758.3529	758.3555	~30
92	4-Cyclopentylpiperazine	$C_{41}H_{45}F_3N_5O_5$ 744.3373	744.3397	<60
93	4-[2-(1-Pyrrolidinyl)ethyl]piperazine	$C_{42}H_{48}F_3N_6O_5$ 773.3638	773.3638	<60

[a] A suspension of 0.05 g (0.064 mmol) of **37** and palladium (5% weight on activated carbon, 0.024 g) in 5 mL of methanol was held under an atmosphere of hydrogen until complete disappearance of **37** as determined by thin layer chromatography (95:5 dichloromethane/methanol eluent). The reaction mixture was filtered to remove the palladium over carbon and the filtrate was evaporated to give 0.04 g of crude **89**. It was purified by column chromatography (95:5 dichloromethane/methanol eluent) to afford 0.011 g (23%) of **89**. HRMS (FAB) calcd for $C_{44}H_{47}F_3N_5O_5$ 782.3534, found 782.3535 $(M+H)^+$.

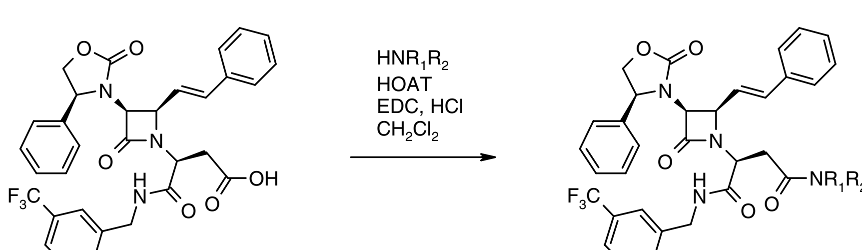

Figure 19. L-Aspartic acid derivatives.

4.1.9.4. 2(*R*)-[[4-(Piperidin-1-yl)piperidin-1-yl]carbonylmethyl]-2-[3(*S*)-(4(*S*)-phenyloxazolidin-2-on-3-yl)-4(*R*)-(2-styryl)azetidin-2-on-1-yl]acetic acid *N*-[(*R*)-α-methylbenzyl]amide (50). Compound **50** was prepared using the procedure shown in Section 4.1.3, except that *N*-benzyloxycarbonyl-D-aspartic acid β-*tert*-butyl ester monohydrate was replaced with **74** and 3-(trifluoromethyl)benzylamine was replaced with 4-(1-piperidinyl)piperidine. Compound **50** was obtained as an off-white solid after flash silica gel column chromatography (CH_2Cl_2 99% and down to 90%/MeOH 1% and up to 10%, NH_4OH <1%). ^1H NMR ($CDCl_3$) δ 1.30–1.52

Table 3. Structures, HRMS (FAB), V1a K_i values

Compound	HNR_1R_2	Calcd for and equal to	Found: (M+H)	K_i (nM)
94	3-(Trifluoromethyl)benzylamine	$C_{44}H_{45}F_3N_5O_5$ 780.3373	780.3344	6100
95	2-(Dimethylamino)ethylamine	$C_{40}H_{49}F_3N_6O_5$ 693.3764	693.3757	>600
96	3-(Dimethylamino)propylamine	$C_{41}H_{51}N_6O_5$ 707.3921	707.3912	>600

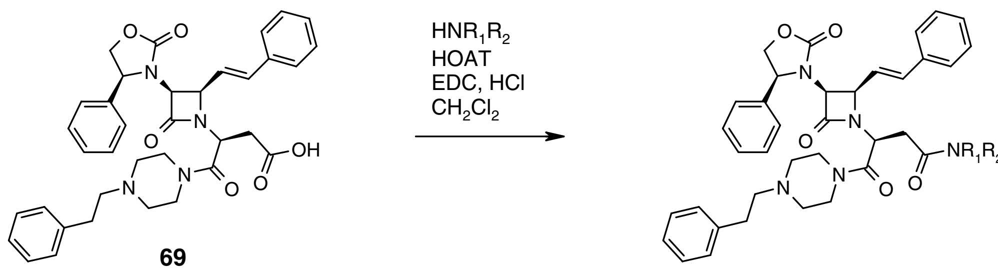

Figure 20. D-Aspartic acid derivatives.

Table 4. Structures and HRMS (FAB), V1a K_i values

Compound	HNR_1R_2	Calcd for and equal to	Found: (M+H)	K_i (nM)
41	4-(1-Piperidinyl)piperidine	$C_{42}H_{47}F_3N_5O_5$ 758.3529	758.3510	1.49
97	4-[(1-Piperidinyl)methyl]piperidine	$C_{43}H_{49}F_3N_5O_5$ 772.3686	772.3666	3.7
98	1-Benzyl-4-amino-piperidine	$C_{44}H_{45}F_3N_5O_5$ 780.3373	780.3353	5.58
99	4-[2-(1-Piperidinyl)ethyl]piperidine	$C_{44}H_{51}F_3N_5O_5$ 786.3842	786.3840	7.9
100	4-(1-Pyrrolidinyl)piperazine	$C_{41}H_{45}F_3N_5O_5$ 744.3373	744.3398	27.5
101	3-(*S*)-(1-Benzyl)-3-amino-pyrrolidine	$C_{43}H_{43}F_3N_5O_5$ 766.3216	766.3223	>30

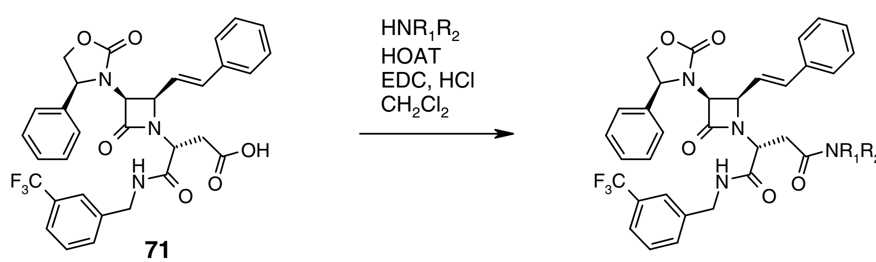

Figure 21. Additional D-aspartic acid derivatives.

Table 5. HRMS (FAB), V1a K_i values

Compound	Calcd for and equal to	Found: (M+H)	K_i (nM)
50	$C_{42}H_{50}N_5O_5$ 704.3812	704.3801	0.30
51	$C_{43}H_{49}F_3N_5O_5$ 772.3686	772.3674	0.66
102	$C_{42}H_{46}F_4N_5O_5$ 776.3435	776.3463	1.13
53	$C_{43}H_{49}F_3N_5O_5$ 772.3686	772.3703	1.27
104	$C_{44}H_{54}N_5O_5$ 732.4125	732.4127	8.7
105	$C_{43}H_{49}F_3N_5O_5$ 772.3686	772.3666	>6
52	$C_{42}H_{50}N_5O_5$ 704.3812	704.3806	>30
103	$C_{44}H_{54}N_5O_5$ 732.4125	732.4108	179

(m, 4H); 1.56–1.72 (m, 7H); 1.81–1.90 (m, 2H); 2.40–2.60 (m, 6H); 2.88–2.96 (m, 1H); 3.14–3.20 (m, 1H); 3.36–3.44 (m, 1H); 3.79–3.86 (m, 1H); 3.99–4.04 (m, 1H); 4.15 (t, $J = 8.3$ Hz, 1H); 4.21 (dd, $J = 5.0$ Hz, $J = 8.0$ Hz, 1H); 4.44–4.55 (m, 1H); 4.60–4.75 (m, 3H); 5.07–5.14 (m, 1H); 6.29–6.36 (m, 1H); 6.74–

6.79 (m, 1H); 7.19–7.46 (m, 15H); 8.23–8.28 (m, 1H). ^{13}C NMR ($CDCl_3$) δ 21.87/21.90, 23.84, 24.90, 26.81, 33.56/33.59, 41.11/41.23, 44.52/44.57, 49.59, 49.67/49.75, 54.97, 55.16, 61.03, 61.77/61.81, 62.43/62.52, 63.37, 70.95, 121.16, 126.30, 126.79, 126.83, 127.25, 128.40, 128.70, 129.63, 129.67, 135.29/135.31, 135.80/135.83, 139.13, 143.93/143.96, 157.96, 163.29, 167.94/167.96, 168.23, 168.51. HRMS (FAB) calcd for $C_{42}H_{50}N_5O_5$ 704.3812, found 704.3801 $(M+H)^+$.

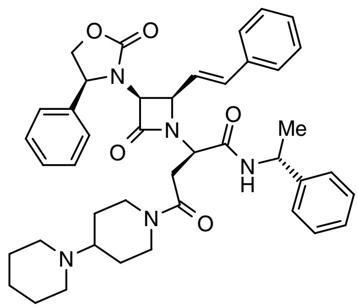

4.1.9.5. 2(*R*)-[[4-[2-(1-Piperidinyl)ethyl]piperidin-1-yl]carbonylmethyl]-2-[3(*S*)-(4(*S*)-phenyloxazolidin-2-on-3-yl)-4(*R*)-(2-styryl)azetidin-2-on-1-yl]acetic acid *N*-[(*R*)-α-methylbenzyl]amide (104). Compound **104** was prepared using the procedure shown in Section 4.1.3', except that *N*-benzyloxycarbonyl-D-aspartic acid β-*tert*-butyl ester monohydrate was replaced with **74** and 3-(trifluoromethyl)benzylamine was replaced with 4-[2-(1-piperidinyl)ethyl]piperidine. Compound **104** exhibited a ^{1}H NMR spectrum consistent with the assigned structure. HRMS (FAB) calcd for $C_{44}H_{54}N_5O_5$ 732.4125, 732.4127 $(M+H)^+$.

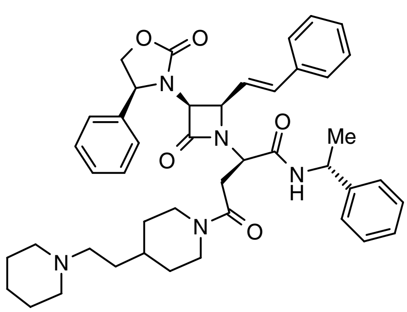

4.1.9.6. 2(*R*)-[[4-(Piperidin-1-yl)piperidin-1-yl]carbonylmethyl]-2-[3(*S*)-(4(*S*)-phenyloxazolidin-2-on-3-yl)-4(*R*)-(2-styryl)azetidin-2-on-1-yl]acetic acid *N*-methyl-*N*-(3-trifluoromethylbenzyl)amide (51). Compound **51** was prepared using the procedure shown in Section 4.1.3, except that *N*-benzyloxycarbonyl-D-aspartic acid β-*tert*-butyl ester monohydrate was replaced with **75** and 3-(trifluoromethyl)benzylamine was replaced with 4-(1-piperidinyl)piperidine. Compound **51** was obtained as an off-white solid after flash silica gel column chromatography (CH_2Cl_2 99% and down to 90%/MeOH 1% and up to 10%, NH_4OH <1%). Compound **51** exhibited a ^{1}H NMR spectrum consistent with the assigned structure. HRMS (FAB) calcd for $C_{43}H_{49}F_3N_5O_5$ 772.3686, found 772.3674 $(M+H)^+$.

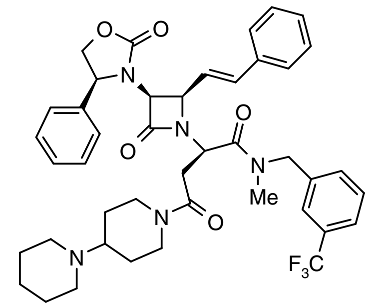

4.1.9.7. 2(*R*)-[[4-(Piperidin-1-yl)piperidin-1-yl]carbonylmethyl]-2-[3(*S*)-(4(*S*)-phenyloxazolidin-2-on-3-yl)-4(*R*)-(2-styryl)azetidin-2-on-1-yl]acetic acid *N*-[(*R*)-α-methyl-3-trifluoromethylbenzyl]amide (53). Compound **53** was prepared using the procedure shown in Section 4.1.3, except that *N*-benzyloxycarbonyl-D-aspartic acid β-*tert*-butyl ester monohydrate was replaced with **77** and 3-(trifluoromethyl)benzylamine was replaced with 4-(1-piperidinyl)piperidine. Compound **53** was obtained as an off-white solid after flash silica gel column chromatography (CH_2Cl_2 99% and down to 90%/MeOH 1% and up to 10%, NH_4OH < 1%). Compound **53** exhibited a ^{1}H NMR spectrum consistent with the assigned structure. HRMS (FAB) calcd for $C_{43}H_{49}F_3N_5O_5$ 772.3686, found 772.3703 $(M+H)^+$.

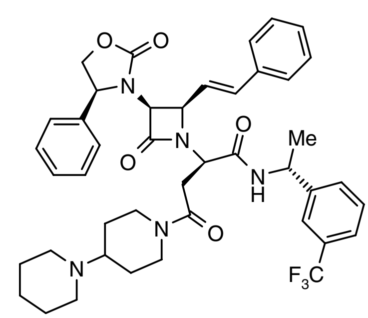

4.1.9.8. 2(*R*)-[[4-(Piperidin-1-yl)piperidin-1-yl]carbonylmethyl]-2-[3(*S*)-(4(*S*)-phenyloxazolidin-2-on-3-yl)-4(*R*)-(2-styryl)azetidin-2-on-1-yl]acetic acid *N*-[(*S*)-α-methyl-3-trifluoromethylbenzyl]amide (105). Compound **105** was prepared using the procedure shown in Section 4.1.3, except that *N*-benzyloxycarbonyl-D-aspartic acid β-*tert*-butyl ester monohydrate was replaced with **76** and 3-(trifluoromethyl)benzylamine was replaced with 4-(1-piperidinyl)piperidine. Compound **105** was obtained as an off-white solid after flash silica gel column chromatography (CH_2Cl_2 99% and down to 90%/MeOH 1% and up to 10%, NH_4OH <1%). Compound **105** exhibited a ^{1}H NMR spectrum consistent with the assigned structure. HRMS (FAB) calcd for $C_{43}H_{49}F_3N_5O_5$ 772.3686, found 772.3666 $(M+H)^+$.

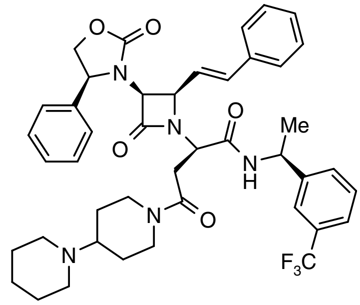

4.1.10. Glutamic acid derivatives. The compounds shown in Table 6, Figure 22 were prepared using the procedure shown in Section 4.1.3, except that *N*-benzyloxycarbonyl-D-aspartic acid β-*tert*-butyl ester monohydrate was replaced with **70**, and 3-(trifluoromethyl)benzylamine was replaced with the appropriate amine HNR_1R_2; all compounds exhibited an ^1H NMR spectrum consistent with the assigned structure.

The compounds shown in Table 7, Figure 23 were prepared using the procedure shown in Section 4.1.3, except that *N*-benzyloxycarbonyl-D-aspartic acid β-*tert*-butyl ester monohydrate was replaced with **79**, and 3-(trifluoromethyl)benzylamine was replaced with the appropriate amine HNR_1R_2; all compounds exhibited an ^1H NMR spectrum consistent with the assigned structure.

The compounds shown in Table 8, Figure 24 were prepared using the procedure shown in Section 4.1.3, except that *N*-benzyloxycarbonyl-D-aspartic acid β-*tert*-butyl ester monohydrate was replaced with **78**, and 3-(trifluoromethyl)benzylamine was replaced with the appropriate amine HNR_1R_2; all compounds exhibited an ^1H NMR spectrum consistent with the assigned structure.

4.2. Biological evaluation

4.2.1. V1a receptor binding assay (Azevan Pharmaceuticals Inc.). A cell line expressing the human V1a receptor in CHO cells (henceforth referred to as the hV1a cell line) was obtained from Dr. Michael Brownstein, NIMH, Bethesda, MD, USA. The hV1a cell culture and cell-based hV1a receptor binding assay were performed according to the methods described by Thibonnier et al.[26] with modifications. The hV1a cell line was grown in alpha-MEM with 10% fetal bovine serum and 250 μg/ml G418 (Gibco, Grand Island, NY, USA). For competitive binding assay, hV1a cells were plated into 12-well culture plate at 1:16 dilution from a confluency flask and maintained in culture for at least two days. Culture medium was then removed, cells were washed with 2 mL binding buffer (25 mM HEPES, 0.25% BSA, 1× DMEM, pH 7.0). To each well, 990 μl binding buffer containing 1 nM [^{3}H]arginine–vasopressin was added, and followed by 10 μl series diluted test compounds dissolved in DMSO. All incubations were in triplicate, and dose-inhibition curves consisted of total binding (DMSO) and 5 concentrations (usually 0.1, 1.0, 10, 100, and 1000 nm) of test agent encompassing the IC_{50}. 100 nM unlabeled arginine–vasopressin (Sigma) was used to assess nonspecific binding. Cells were incubated for 30 min at 37 °C, assay mixture was removed, and each well was washed three times with PBS (pH 7.4). SDS (1 mL, 2%) was added per well and plates were let sit for 30 min. The whole content in a well was transferred to a scintillation vial. Each well was rinsed with 0.5 mL PBS, which was then added to the corresponding vial. Scintillation fluid (Ecoscint, National Diagnostics, Atlanta, Georgia) was then added at 3 mL per vial. Samples were counted in a liquid scintillation counter (Beckman LS6500). IC_{50} values were calculated by Prism Curve fitting software. The conversion factor for computing K_i from IC_{50} was 0.61.

4.2.2. V1a receptor binding assay (Eli Lilly & Co). The V1a binding assay employed at Eli Lilly used the same cell line expressing the human V1a receptor in CHO cells, but the assay differed inasmuch as binding was carried out on membranes using a filtration method.[22] IC_{50} values measured by the two methods usually differed by 2-fold or less.

4.2.3. Measurement of plasma and brain levels in dogs after oral dosing. Samples were collected from a single dog dosed orally with compound at 10 mg/kg in 10% DMSO/90% PEG300. Blood and brain samples (cortex, brain stem, cerebellum, hypothalamus, and hippocampus regions) were harvested and frozen in liquid nitrogen and stored at −70 °C prior to analysis by LC/MS mass spectrometry. Samples were thawed on ice, homogenized in pH 9.4 buffer on ice and extracted with ethyl acetate after addition of a reference compound to measure extraction efficiency. Extracts were removed and taken to dryness, reconstituted in acetonitrile and injected on a Finnigan ESI LC/MS/MS system. Spiked control brain samples

Table 6. Structures, HRMS (FAB), V1a IC_{50} and K_i values

Compound	HNR_1R_2	Calcd for and equal to	Found: (M+H)	K_i (nM)
48	4-Cyclohexylpiperazine	$C_{43}H_{49}F_3N_5O_5$ 772.3686	772.3672	0.27
106	4-(Cyclohexylmethyl)piperazine	$C_{44}H_{51}F_3N_5O_5$ 786.3842	786.3862	0.46
46	4-(2-Phenylethyl)piperazine	$C_{45}H_{47}F_3N_5O_5$ 794.3529	794.3502	1.17
47	4-(1-Piperidinyl)piperidine	$C_{43}H_{49}F_3N_5O_5$ 772.3686	772.3685	1.45
107	4-Propylpiperazine	$C_{40}H_{45}F_3N_5O_5$ 732.3373	732.3371	1.19
108	4-[(1-Piperidinyl)methyl]piperidine	$C_{44}H_{51}F_3N_5O_5$ 786.3842	786.3821	1.95
109	2-(1-Piperidinyl)ethylamine	$C_{40}H_{45}F_3N_5O_5$ 732.3373	732.3374	9
110	4-[2-(1-Piperidinyl)ethyl]piperidine	$C_{45}H_{53}F_3N_5O_5$ 800.3999	800.4019	9.9

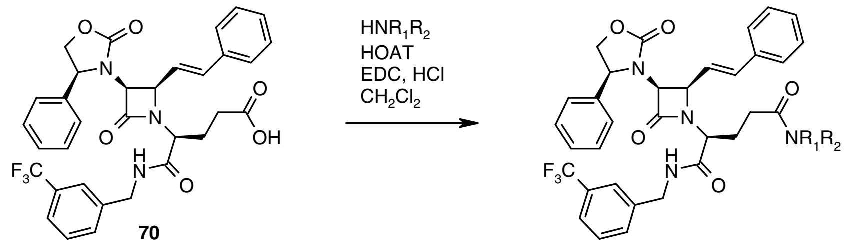

Figure 22. L-Glutamic acid derivatives.

Table 7. Structures, HRMS (FAB), V1a K_i values

Compound	HNR_1R_2	Calcd for and equal to	Found (M+H)	K_i (nM)
111	2-Fluoro-3-(trifluoromethyl)benzylamine	$C_{43}H_{48}F_4N_5O_5$ 790.3592	790.3572	0.20
112	2,3-Dichlorobenzylamine	$C_{42}H_{48}Cl_2N_5O_5$ 772.3033	772.3011	0.38
113	2-Fluoro-5-(trifluoromethyl)benzylamine	$C_{43}H_{48}F_4N_5O_5$ 790.3592	790.3568	0.41
114	3-Fluoro-5-(trifluoromethyl)benzylamine	$C_{43}H_{48}F_4N_5O_5$ 790.3592	790.3577	0.51
115	3-Chlorobenzylamine	$C_{42}H_{49}ClN_5O_5$ 738.3422	738.3441	0.66
116	3,5-Difluorobenzylamine	$C_{42}H_{48}F_2N_5O_5$ 740.3624	740.3624	0.82
117	2-(Trifluoromethyl)benzylamine	$C_{43}H_{49}F_3N_5O_5$ 772.3686	772.3692	0.93
118	3,5-Bis-(trifluoromethyl)benzylamine	$C_{44}H_{48}F_6N_5O_5$ 840.3560	840.3583	4.45
119	4-Fluoro-3-(trifluoromethyl)benzylamine	$C_{43}H_{48}F_4N_5O_5$ 790.3592	790.3588	<30

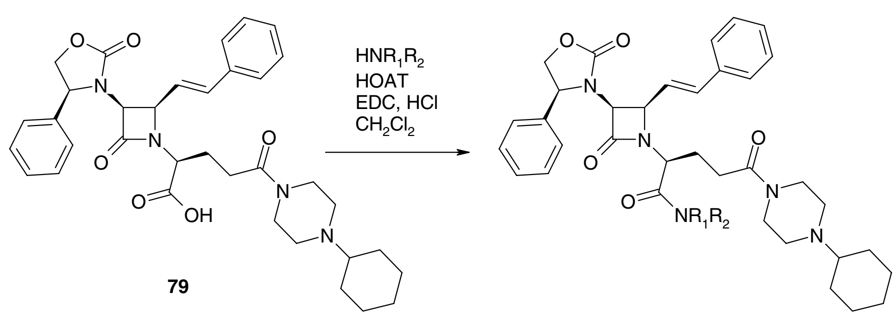

Figure 23. Additional L-glutamic acid derivatives.

Table 8. Structures, HRMS (FAB), V1a K_i values

Compound	HNR_1R_2	Calcd for and equal to	Found (M+H)	K_i (nM)
49	4-Cyclohexylpiperazine	$C_{43}H_{49}F_3N_5O_5$ 772.3686	772.3707	5.84
120	4-Butylpiperazine	$C_{41}H_{47}F_3N_5O_5$ 746.3529	746.3503	10.5
121	4-Isopropylpiperazine	$C_{40}H_{45}F_3N_5O_5$ 732.3373	732.3347	13
122	4-(2-Phenylethyl)piperazine	$C_{45}H_{47}F_3N_5O_5$ 794.3529	794.3552	33
123	4-(Cyclohexylmethyl)-piperazine	$C_{44}H_{51}F_3N_5O_5$ 786.3842	786.3823	>12
124	4-(1-Piperidinyl)piperidine	$C_{43}H_{49}F_3N_5O_5$ 772.3686	772.3688	~30

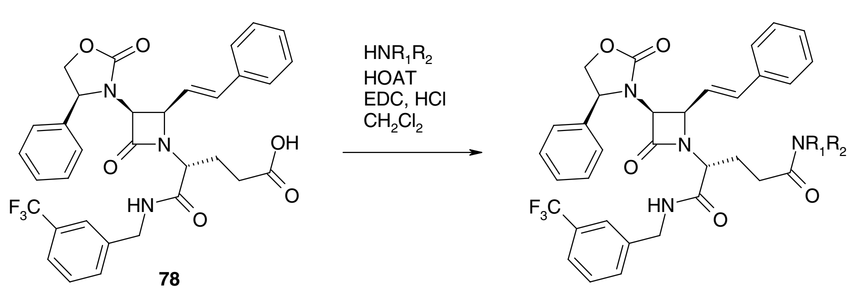

Figure 24. D-Glutamic acid derivatives.

were prepared in similar fashion for use as quantitation standards.

4.2.4. Measurement of plasma and brain levels in rats after oral dosing. Initial experiments showed that in most cases our compounds could be dissolved at 20 mg/ml in 23% hydroxypropyl β-cyclodextrin with 0.68% lactic acid. Sprague–Dawley rats (Charles River Laboratory) were dosed by gavage with a combination of three compounds (20 mg/kg each): **22** + **41** + **48** or **42** + **46** + **47**. Blood (approximately 3 mL) was collected from three animals per group per time point at 0.25, 0.5, 1, 2, 4, 8, 12, and 24 h post-dose. Blood was collected via exsanguination (cardiac puncture) under carbon dioxide anesthesia into tubes containing sodium heparin anticoagulant and plasma was separated by centrifugation within 1 h. Brains were collected at the same time points. Plasma and brain levels were determined by LC/MS/MS.

Acknowledgments

We thank Norman Mason and Anne Van Abbema for carrying out vasopressin binding experiments at Lilly, and Elizabeth Lutz and Harlan Shannon for help with the cyclodextrin/lactic acid formulation. This work was supported by NIH Grants HD37290 to N.G.S. and MH063663 to G.A.K.

References and notes

1. Jard, S.; Elands, J.; Schmidt, A.; Barberis, C. In *Progress in Endocrinology*; Imura, H., Shizume, K., Eds.; Elsevier: Amsterdam, 1998; pp 1183–1189.
2. Birnbaumer, M.; Seibold, A.; Gilbert, S.; Ishido, M.; Barberis, C.; Antaramian, A.; Brabet, P.; Rosenthal, W. *Nature* **1992**, *357*, 333.
3. Kimura, T.; Tanizawa, O.; Mori, K.; Brownstein, M. J.; Okayama, H. *Nature* **1992**, *356*, 526.
4. Morel, A.; O'Carroll, A. M.; Brownstein, M. J.; Lolait, S. J. *Nature* **1992**, *356*, 523.
5. Sugimoto, T.; Saito, M.; Mochizuki, S.; Watanabe, Y.; Hashimoto, S.; Kawashima, H. *J. Biol. Chem.* **1994**, *269*, 27088.
6. Mahlmann, S.; Meyerhof, W.; Hausmann, H.; Heierhorst, J.; Schönrock, C.; Zwiers, H.; Lederis, K.; Richter, D. *Proc. Natl. Acad. Sci. U.S.A.* **1994**, *91*, 1342.
7. Van Kesteren, R. E.; Tensen, C. P.; Smit, A. B.; Van Minnen, J.; Van Soest, P. F.; Kits, K. S.; Meyerhof, W.; Richter, D.; Van Heerikhuizen, H.; Vreugdenhil, E.; Geraerts, W. P. M. *Neuron* **1995**, *15*, 897.
8. Ring, R. H. *Curr. Pharm. Des.* **2005**, *11*, 205.
9. Landgraf, R. *CNS Neurol. Disord. Drug Targets* **2006**, *5*, 167.
10. Tahara, A.; Tsukada, J.; Tomura, Y.; Kusayama, T.; Wada, K.; Ishii, N.; Taniguchi, N.; Suzuki, T.; Yatsu, T.; Uchida, W.; Shibasaki, M. *Pharmacol. Res.* **2005**, *51*, 275.
11. Xiang, M. A.; Chen, R. H.; Demarest, K. T.; Gunnet, J.; Look, R.; Hageman, W.; Murray, W. V.; Combs, D. W.; Patel, M. *Bioorg. Med. Chem. Lett.* **2004**, *14*, 2987.
12. Derdowska, I.; Prahl, A.; Kowalczyk, W.; Janecki, M.; Melhem, S.; Trzeciak, H. I.; Lammek, B. *Eur. J. Med. Chem.* **2005**, *40*, 63.
13. Serradeil-Le Gal, C.; Derick, S.; Brossard, G.; Manning, M.; Simiand, J.; Gaillard, R.; Griebel, R.; Guillon, G. *Stress* **2003**, *6*, 199.
14. Shimada, Y.; Taniguchi, N.; Matsuhisa, A.; Akane, H.; Kawano, N.; Suzuki, T.; Tobe, T.; Kakefuda, A.; Yatsu, T.; Tahara, A.; Tomura, Y.; Kusayama, T.; Wada, K.; Tsukada, J.; Orita, M.; Tsunoda, T.; Tanaka, A. *Bioorg. Med. Chem Lett.* **2006**, *14*, 1827.
15. Galanski, M. E.; Erker, T.; Studenik, C. R.; Kamyar, M.; Rawnduzi, P.; Pabstova, M.; Lemmens-Gruber, R. *Eur. J. Pharm. Sci.* **2005**, *24*, 421.
16. This argument is very similar to the concept underlying 'privileged fragments' Evans, B. E.; Rittle, K. E.; Bock, M. F. G.; Dipardo, R. M.; Friedinger, R. M.; Whiter, W. L.; Lundell, G. F.; Veber, D. F.; Anderson, P. S.; Chang, R. S. L.; Lotti, V. J.; Cerino, D. J.; Chen, T. B.; Kling, P. J.; Kunkel, K. A.; Springer, J. P.; Hirshfield, J. *J. Med. Chem.* **1988**, *31*, 2235.
17. A second potential approach is implicit in the weak (suboptimal) binding of beta to A in Figure 1. By screening weak binders to a related receptor (A), one could find strong binders to the target receptor (B). Pairwise comparisons of results for NK-2, NPY1, BK2, and V1a screening of the Neuropeptide Cassette confirm this hypothesis: prescreening for weak activity at any one of the four targets resulted in 4- to 7-fold enrichments in hit rates for the other three targets (RFB, unpublished results). LY307174 itself had weak but detectable affinity (IC_{50} ~40 μM) at the hamster NK-2 receptor.
18. De, B.; Plattner, J. J.; Bush, E. N.; Jae, H. S.; Diaz, G.; Johnson, E. S.; Perun, T. J. *J. Med. Chem.* **1989**, *32*, 2036.
19. Evans, D. A.; Sjogren, E. B. *Tetrahedron Lett.* **1985**, *26*, 3783.
20. Evans, D. A.; Sjogren, E. B. *Tetrahedron Lett.* **1985**, *26*, 3787.
21. X-ray resolution and ORTEP of **7** provided as a pdf file.
22. Bruns, R. F.; Cooper, R. D. G.; Dressman, B. A.; Hunden, D. C.; Kaldor, S. W.; Koppel, G. A.; Rizzo, J. R.; Skelton, J. J.; Steinberg, M. I. U.S. Patent 6,204,260, 2001.
23. Hipskind, P. A.; Howbert, J. J.; Bruns, R. F.; Foreman, M. M.; Gehlert, D. R.; Iyengar, S.; Phebus, L. A.; Regoli, D.; Cho, S. S. Y.; Crowell, T. A.; Johnson, K. W.; Krushinski, J. H.; Li, D. L.; Lobb, K. L.; Mason, N. R.; Muehl, B. S.; Nixon, J. A.; Simmons, R. M.; Threlkeld, P. G.; Waters, D. C.; Gitter, B. D. *J. Med. Chem.* **1996**, *39*, 736.
24. The other four compounds tested for plasma and brain levels were **42**, **46**, **47**, and **48**.
25. Evans, D. A.; Sjobren, E. B. U.S. Patent 4,665,171, 1987.
26. Thibonnier, M.; Auzan, C.; Madhun, Z.; Wilkins, P.; Berti-Mattera, L.; Clauser, E. *J. Biol. Chem.* **1994**, *269*, 3304.